Herschel's view of of the atomic and molecular content of Herbig Ae/Be discs

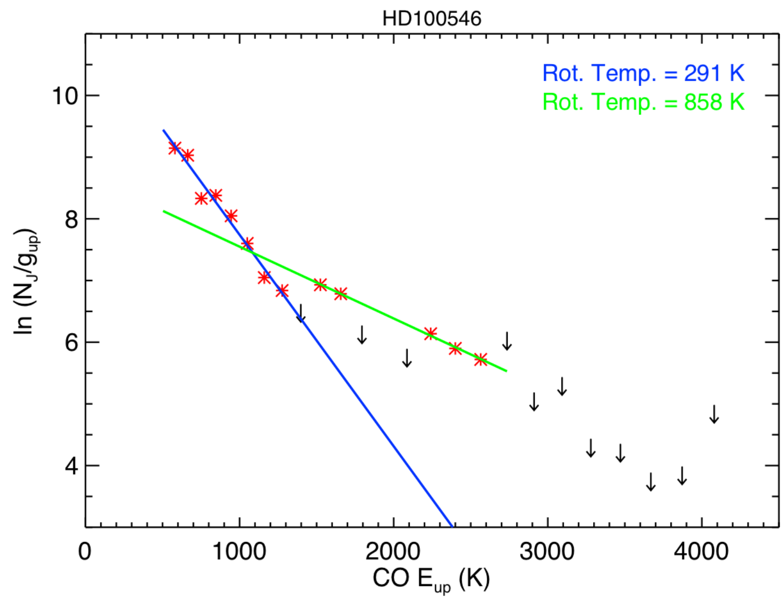

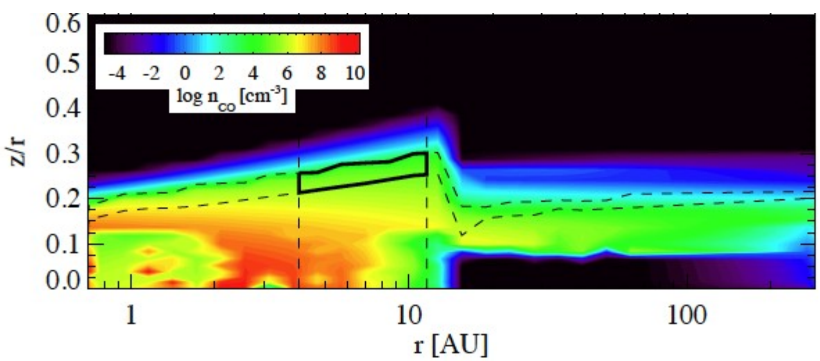

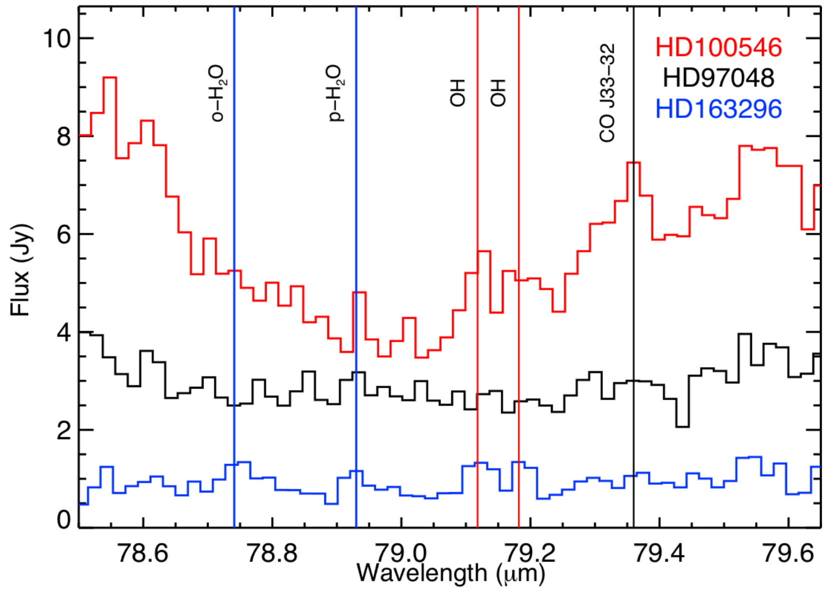

Gwendolyn Meeus, UAM Madrid

Outline

Herbig Ae stars

- Correlations with [OI]
- CO ladders
- Other detected lines
- Disc modelling

Herbig Be stars

Conclusions

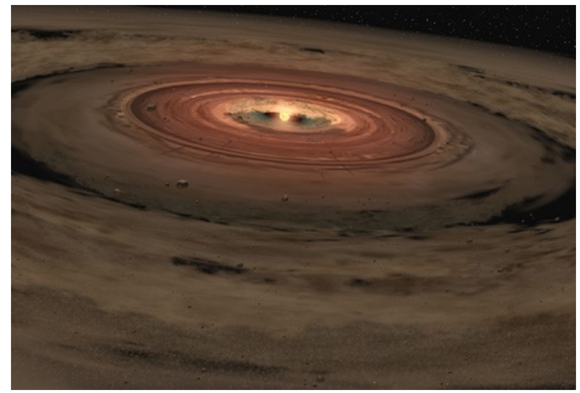

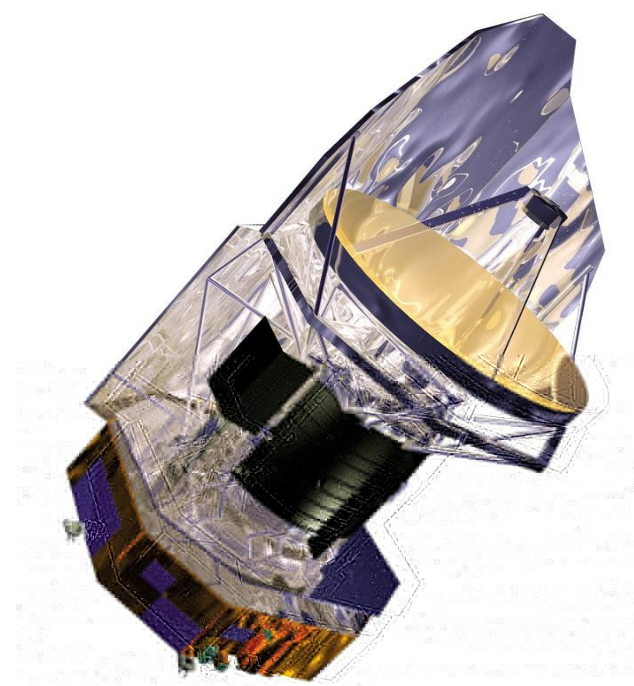

Herschel Space Observatory

3.5m mirror! Phot. & spec. 55 to 672 μm.

2 OT Key Projects on protoplanetary discs:

GASPS PI: *B. Dent*

S. Brittain, C. Eiroa, C.A. Grady, C. Howard, I. Kamp, C. Martin-Zaïdi, G. Mathews, F. Ménard, I. Mendigutía, B. Montesinos, C. Pinte, A. Roberge, G. Sandell, W.-F. Thi, B. Vandenbussche and J.P. Williams

DIGIT PI: *N. Evans*

J. Bouwman, S. Bruderer, E. van Dishoeck, C. Dominik, D. Fedele, J. Green, M. Güdel, G. Herczeg, Th. Henning, J.-E. Lee, K. Maaskant, B. Merin, G. Mulders, J. Najita, C. Salyk, B. Sturm, and R. Waters

Continuum observations: tracing different regions in disc

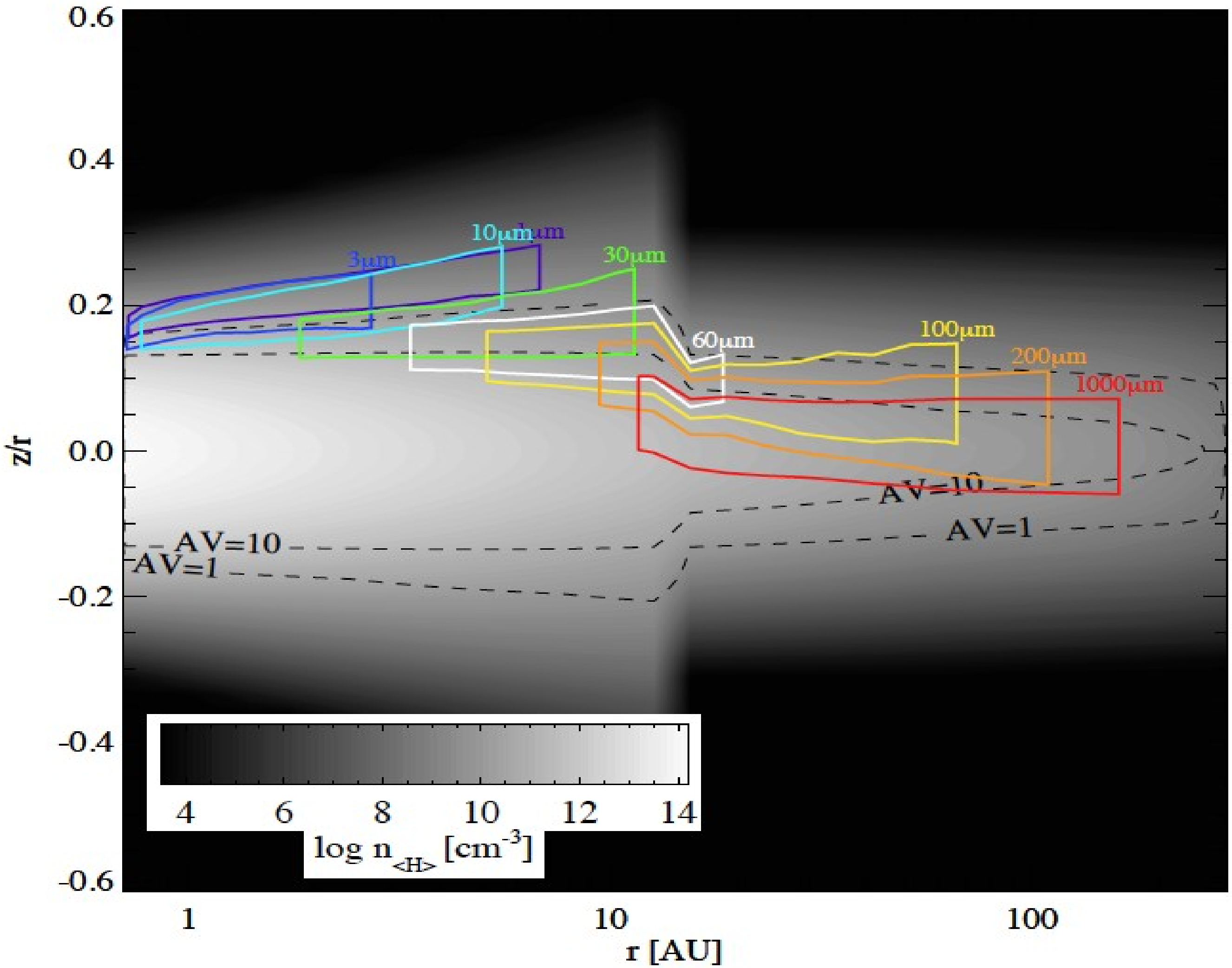

The longer the wavelength, the further away from the star and the deeper in the disc the emission originates

Different gas species & transitions trace different regions in disc

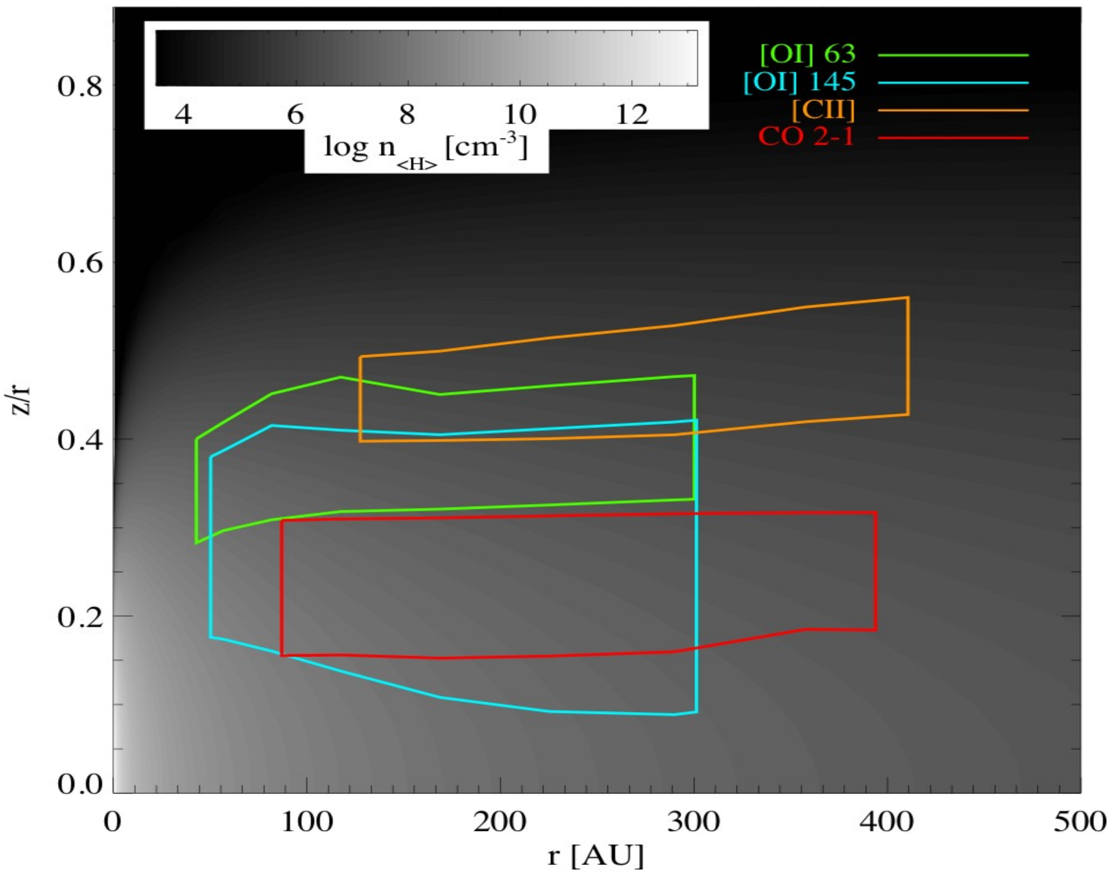

Important transitions in far-IR

-Fine structure lines of atoms:

[OI] 63.2 and 145.5 µm
[CII] 157.7 µm

-Rotational lines of molecules:

CO middle to high J-lines
OH ($OH + H_2 \rightarrow H_2O + H$)
H_2O, CH^+

Far-IR lines trace gas in the *OUTER DISC*

The Herbig Ae sample at [OI] 63.2 micron: variety in strength

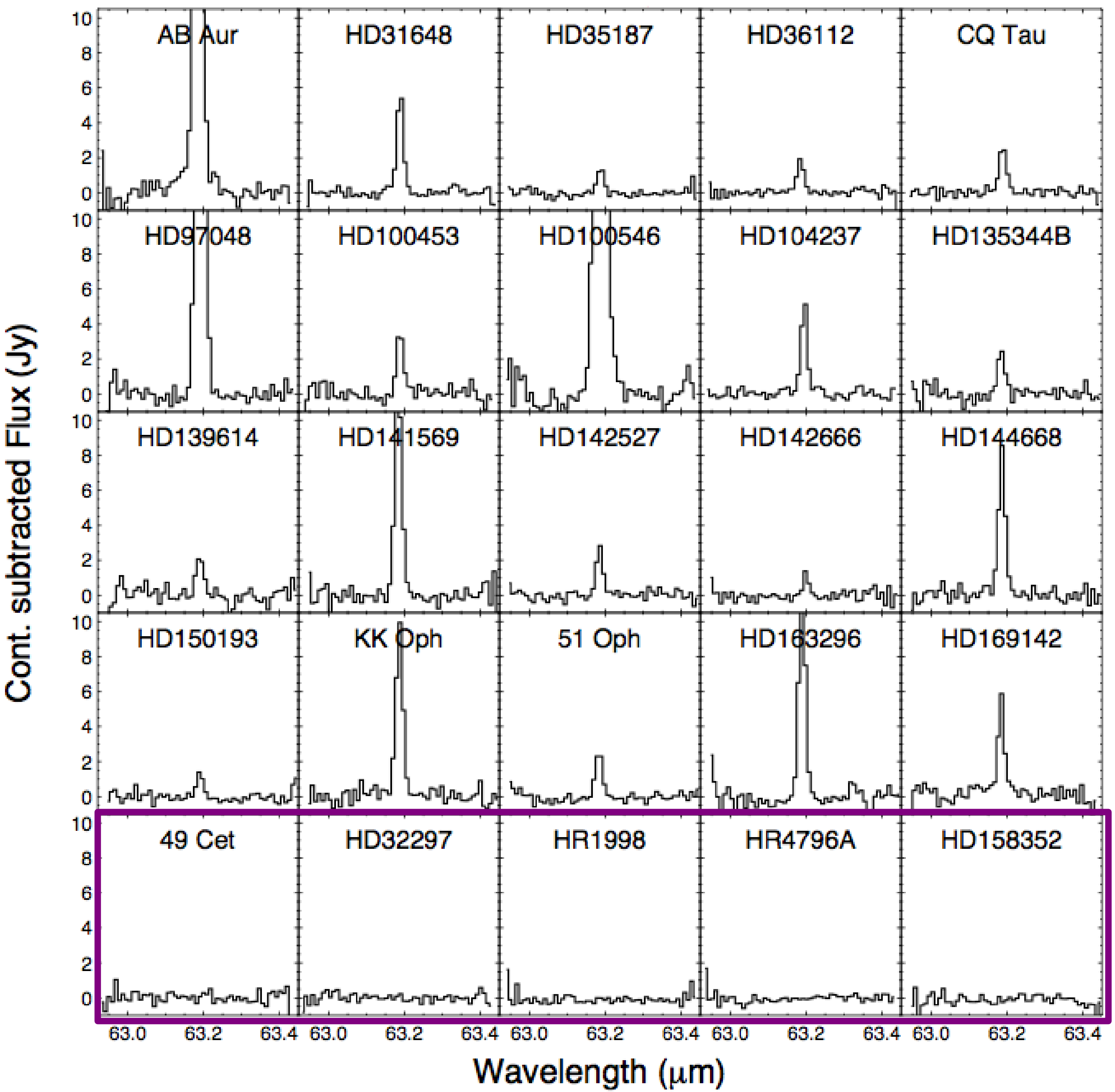

Debris discs

Trends with [OI] 63 μm line flux

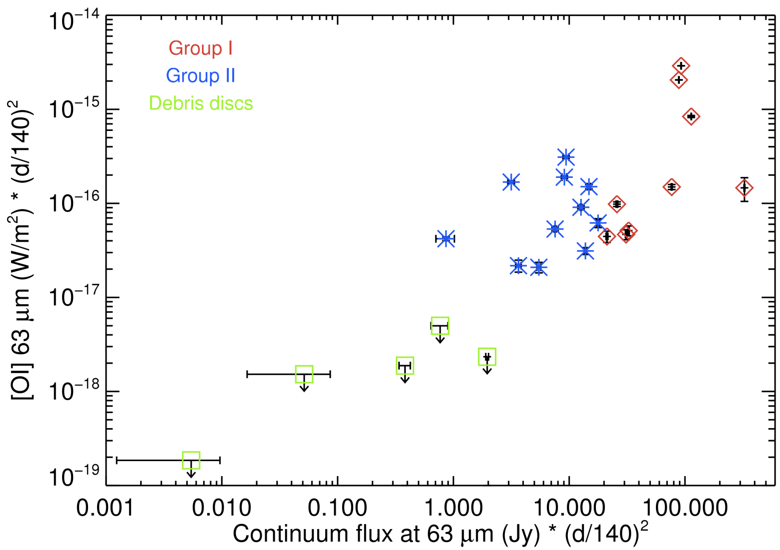

FIR continuum

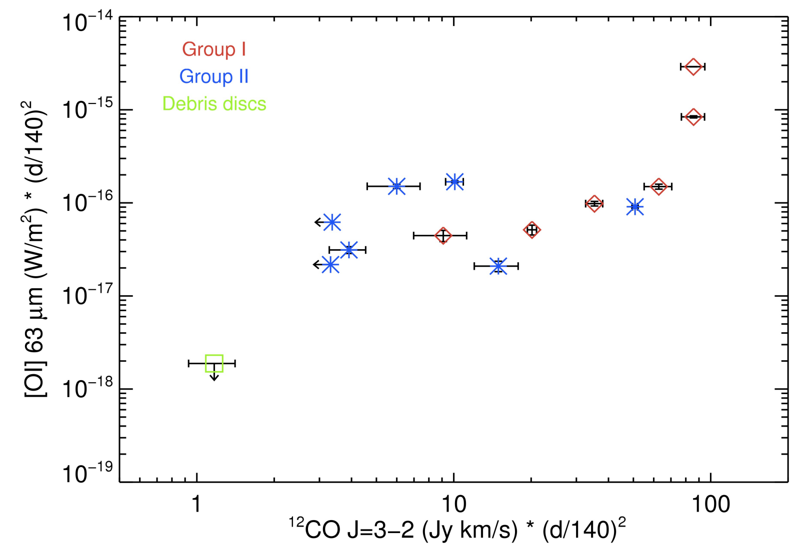

^{12}CO J=3-2 Cold Gas

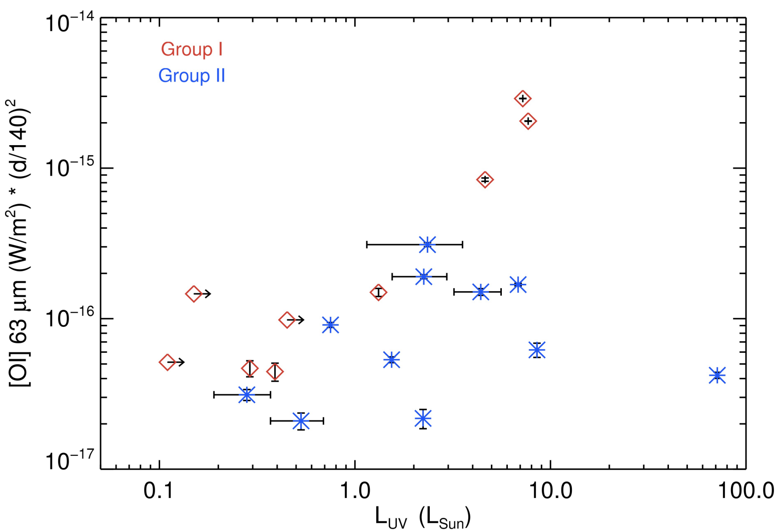

[OI] versus L_{UV}

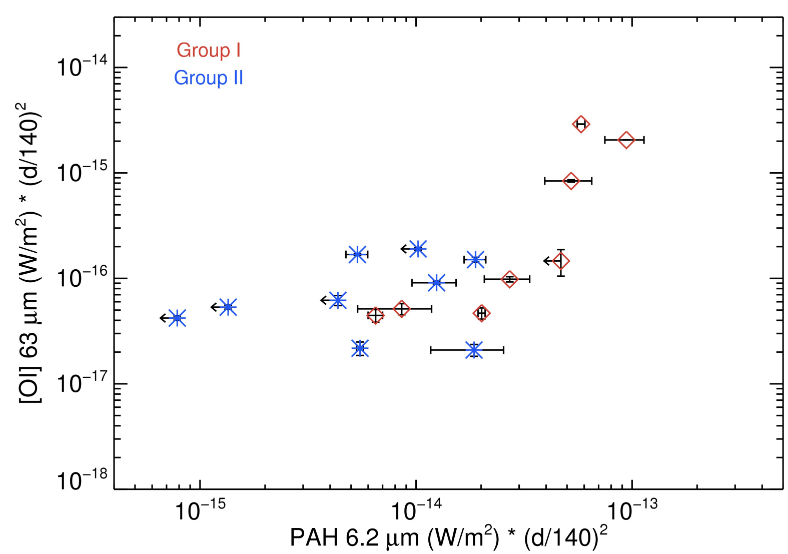

[OI] versus L_{PAH}

[OI] vs. Accretion indicators

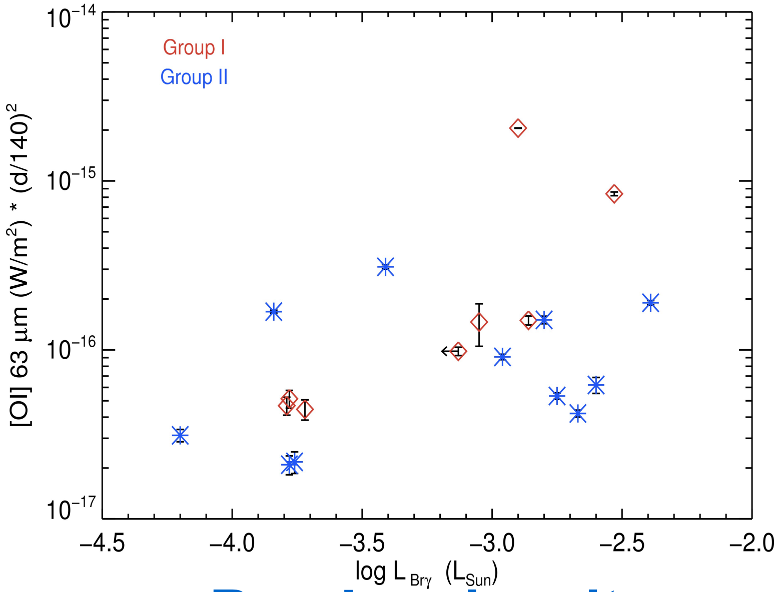

Brγ Luminosity

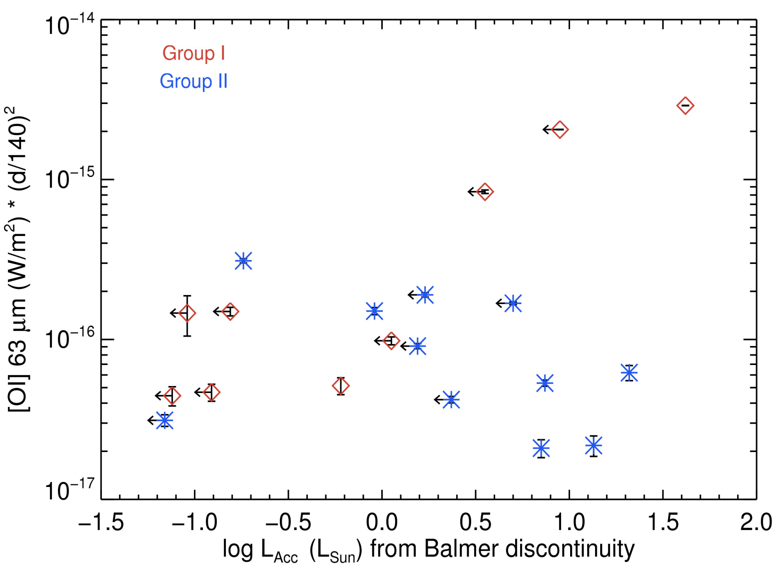

Balmer Excess

! Acc. contributes little to L_{UV} in HAEBEs

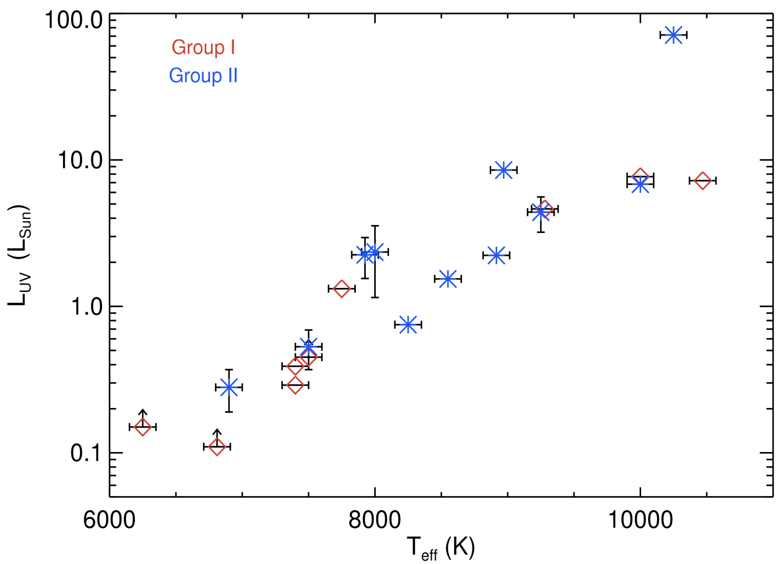

[OI] 63 μm vs. X-ray Luminosity

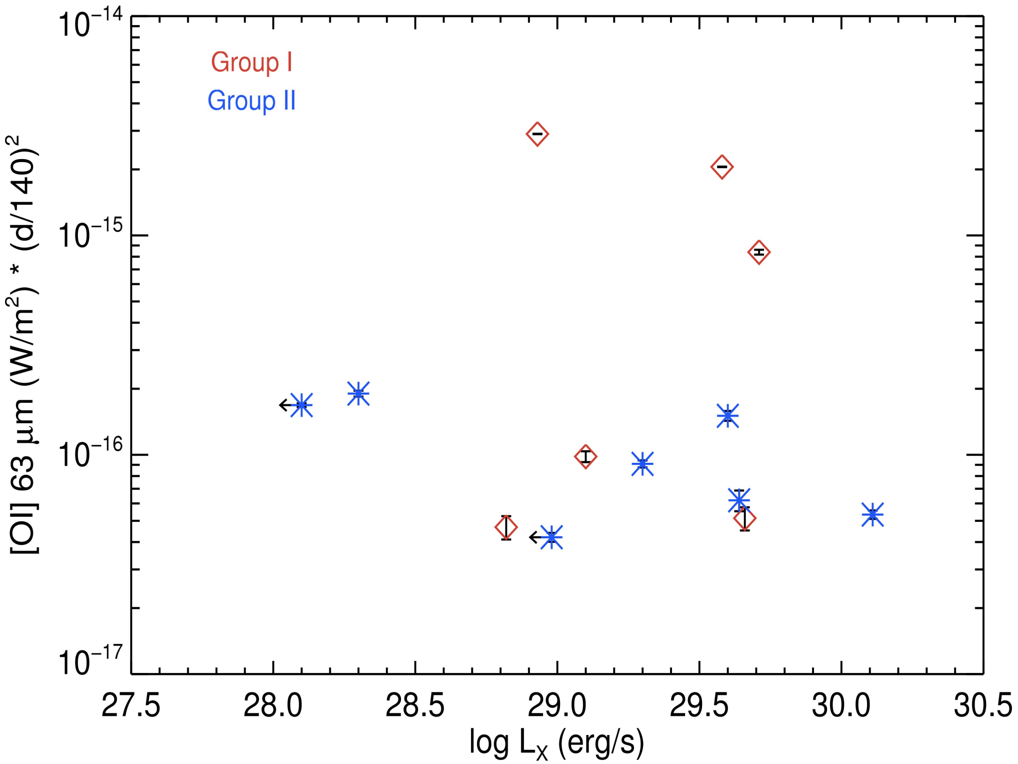

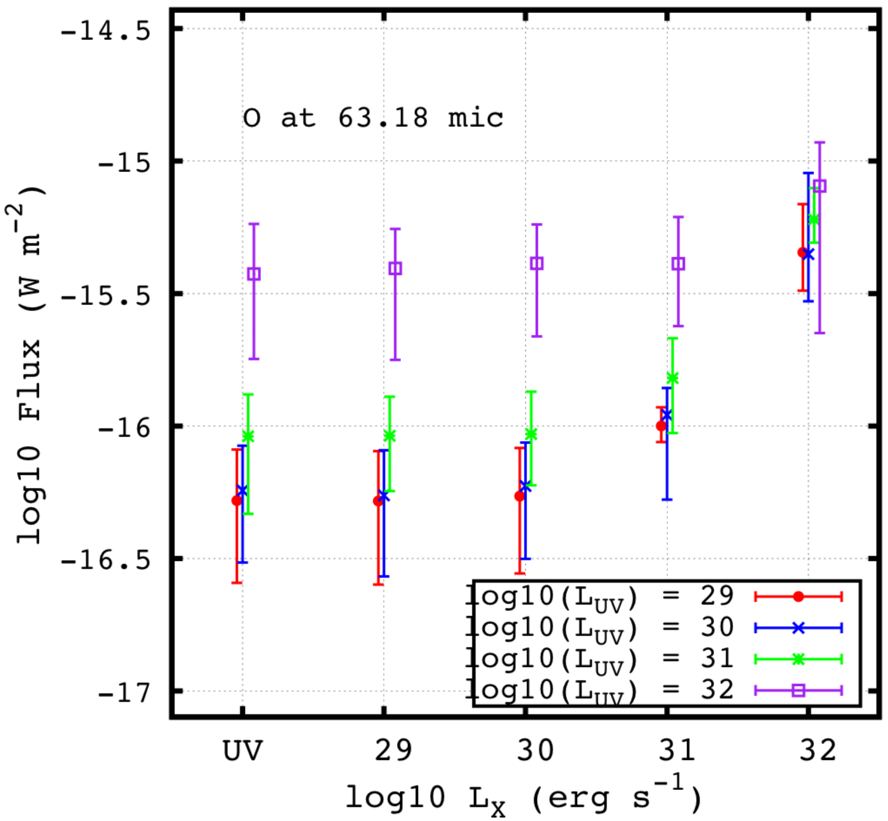

[OI] versus L_X

Predicted Line flux

Aresu et al. 2011, 2012

[OI] 145 μm: less frequent

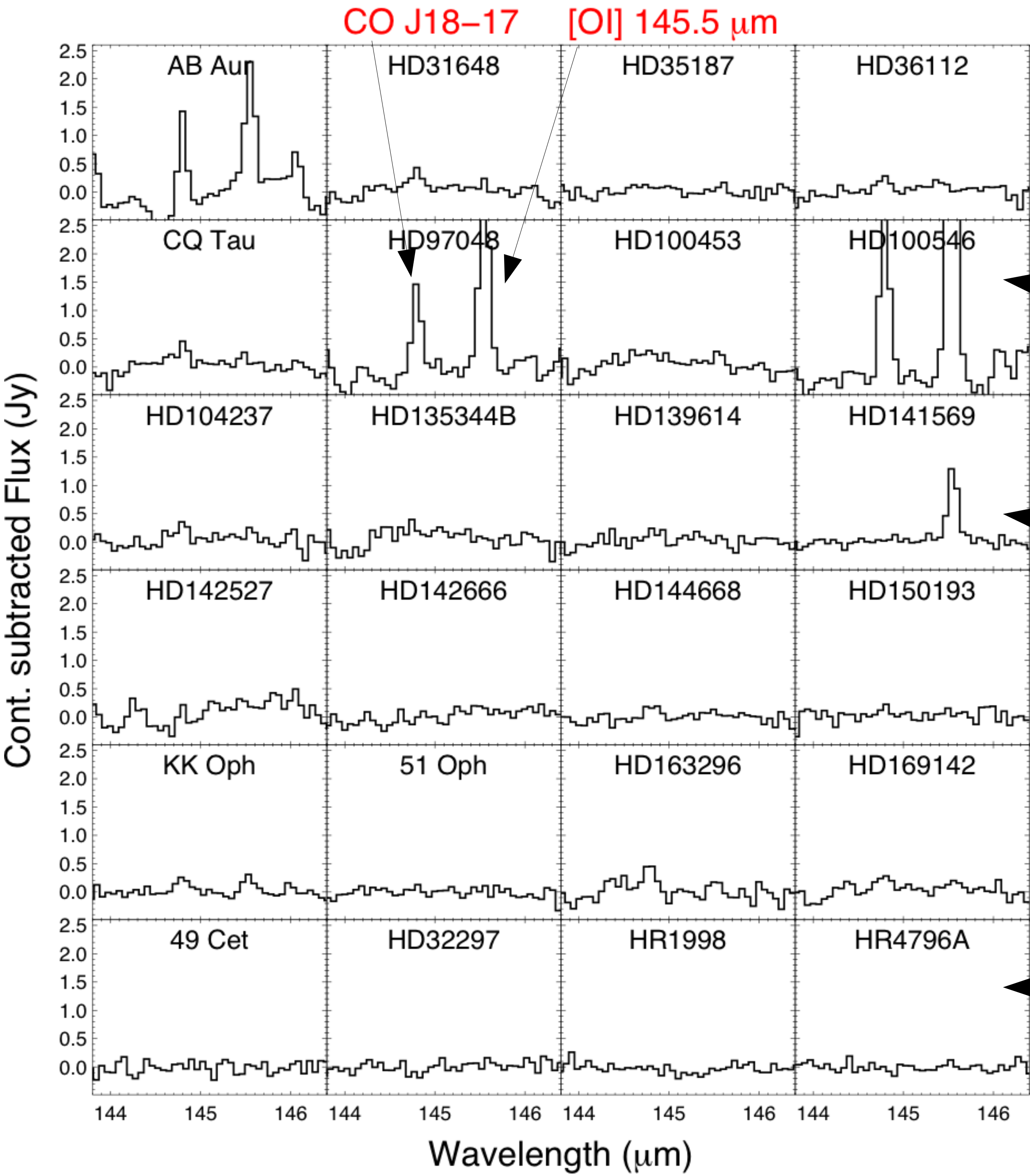

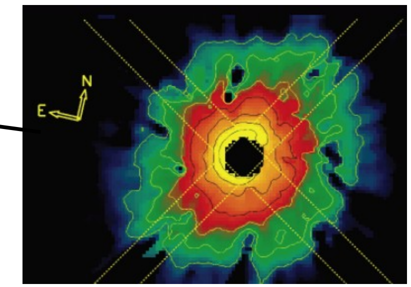

Gap,
hot wall

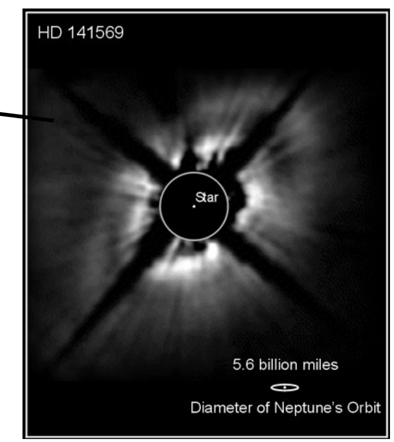

A lot of gas
dissipated
Transitional

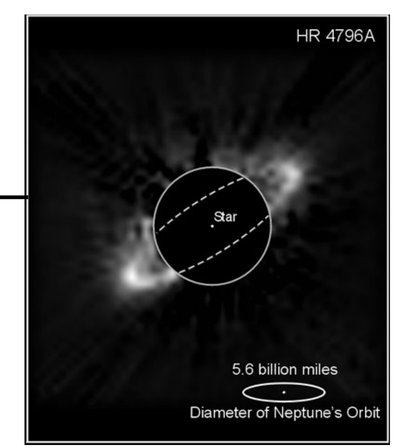

Debris disc

Carbonmonoxide: transitions

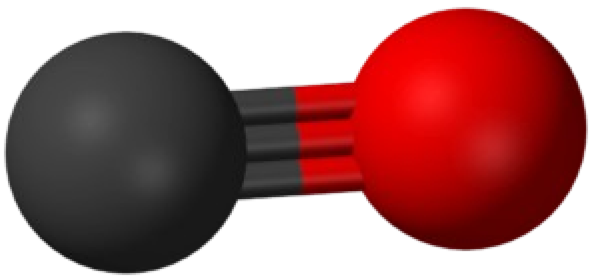

Δ J = +/- 1 (R/P branch)

Cold gas (T ~ 30 K) at far-IR/submm
pure rotational Δ v = 0

Hot gas (T ~ 2000 K) at 4.7 μm:
ro-vibrational fundamental Δ v = 1

Warm gas (T ~ 1000 K) at 2.3 μm:
ro-vibrational overtone Δ v = 2

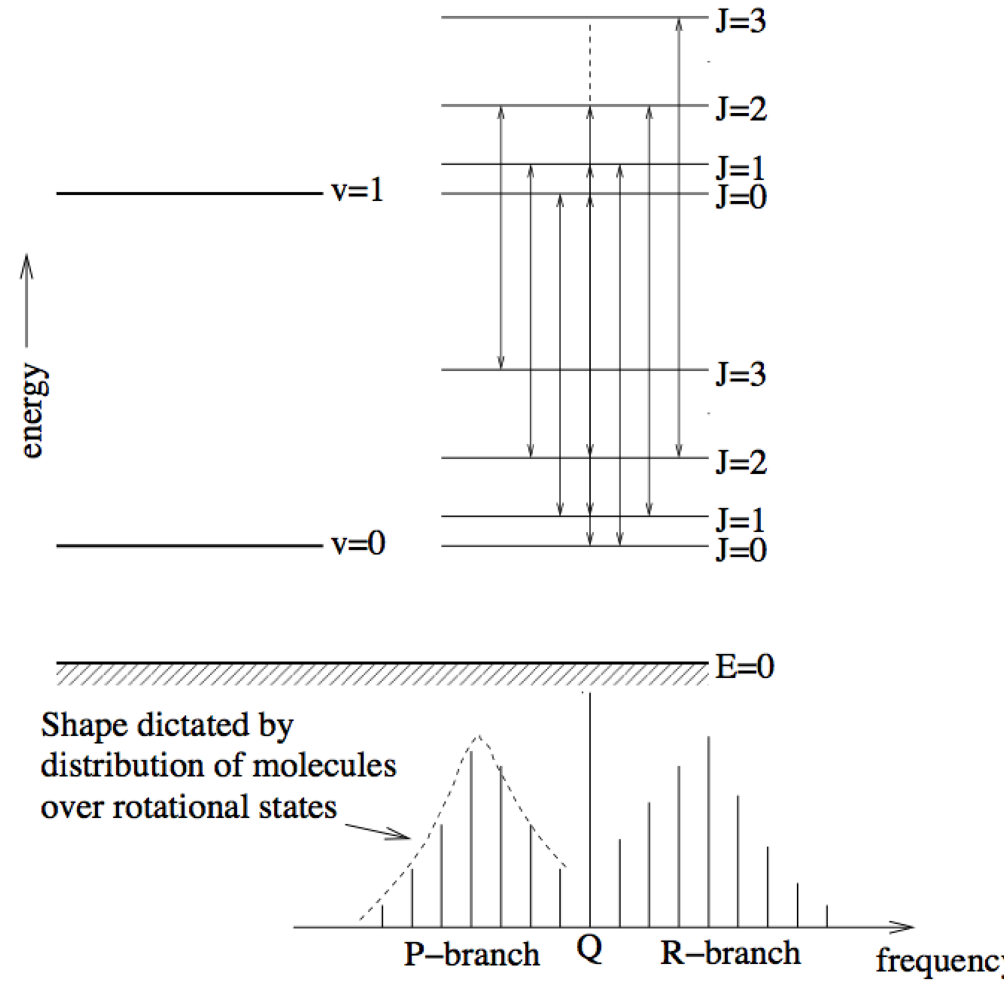

CO lines: great gas disc diagnostics

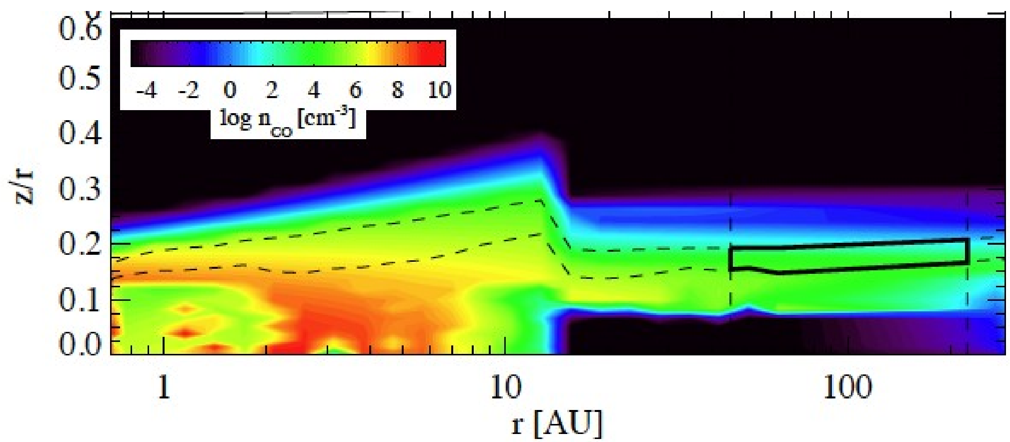

CO 1300 μm
Pure
rotational
J=2-1

CO 144.78 μm
Pure rotational
J=18-17

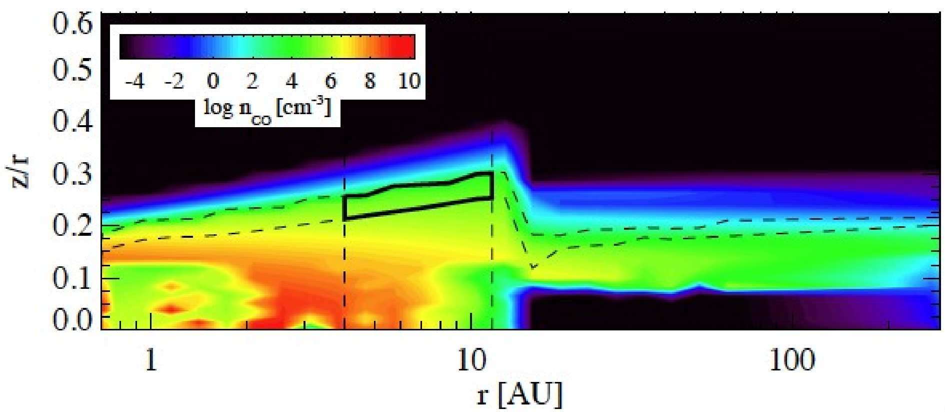

CO 4.844 μm
Fundamental
Ro-Vibrational. lines

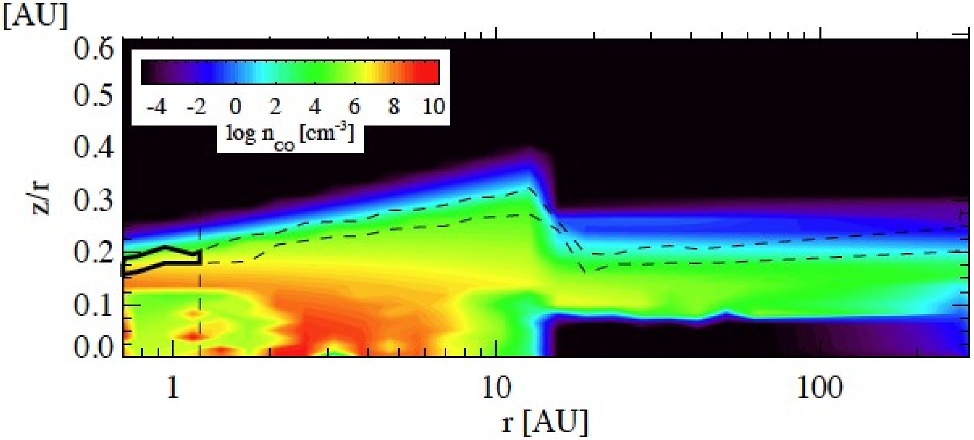

PACS range spec. observations: 55 to 200 μm; CO detections: J=30-29 down to 14-13

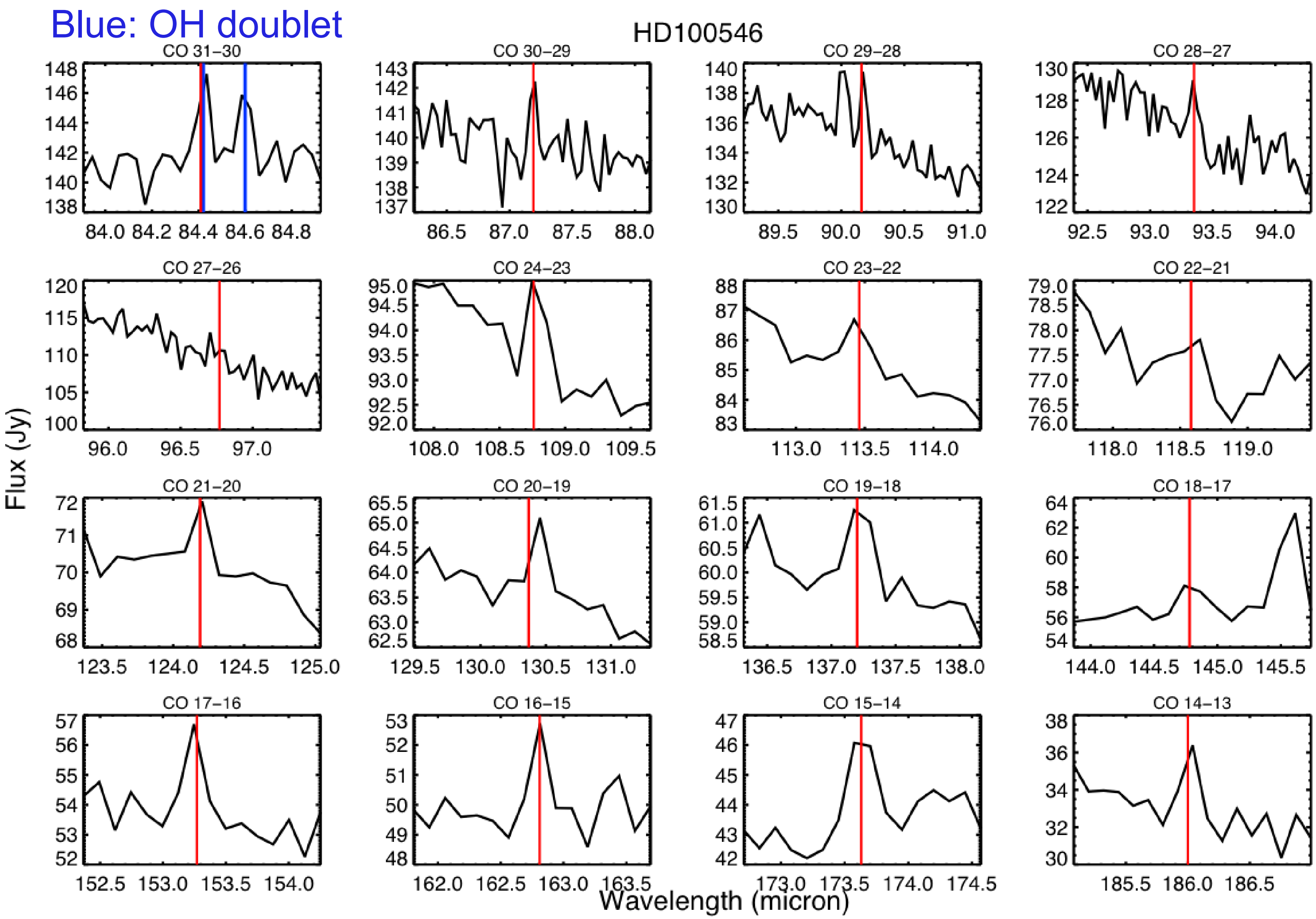

Rotational diagrams: single T_{rot} ~ 200-300 K

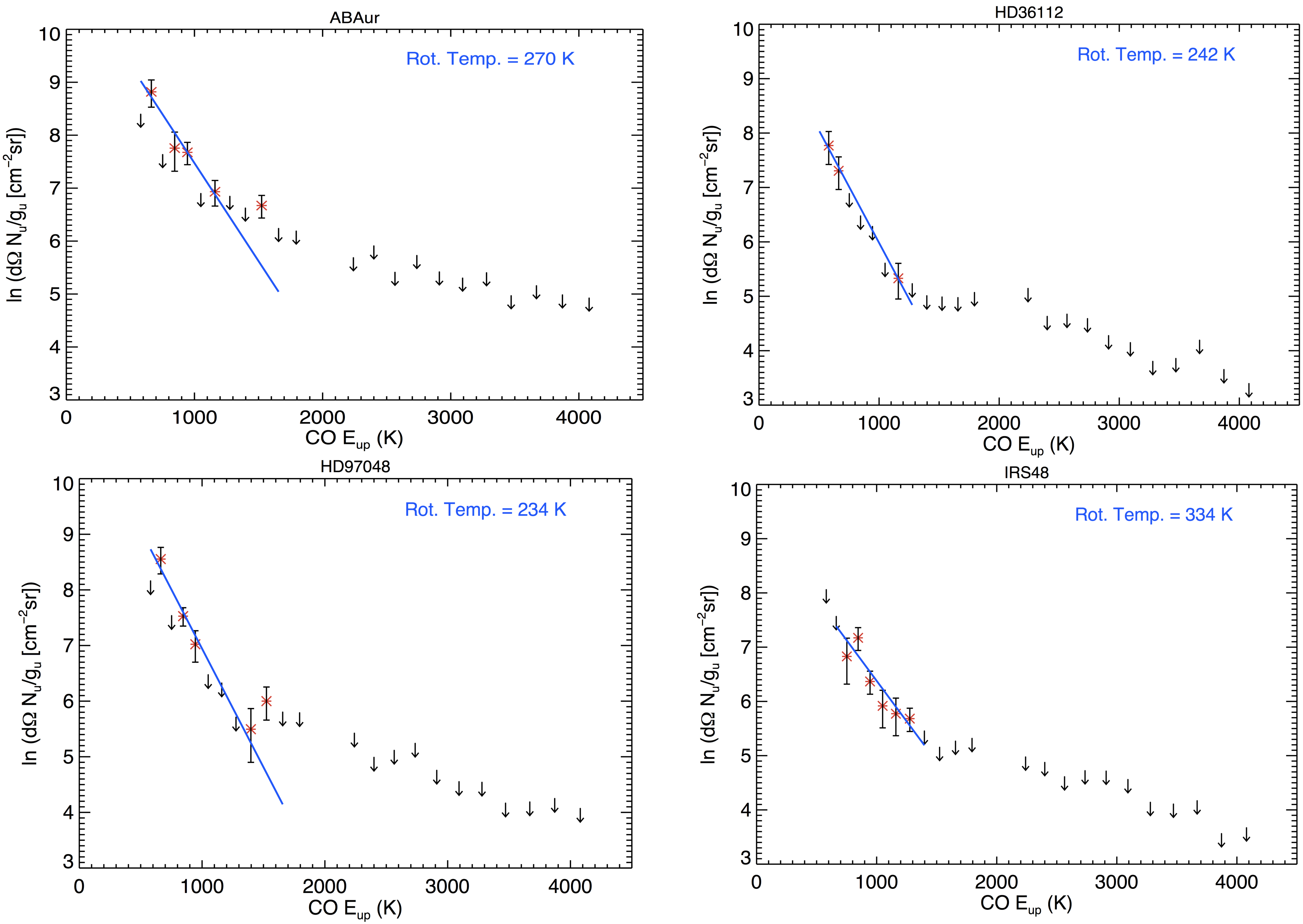

But HD100546 needs both a warm and hot component

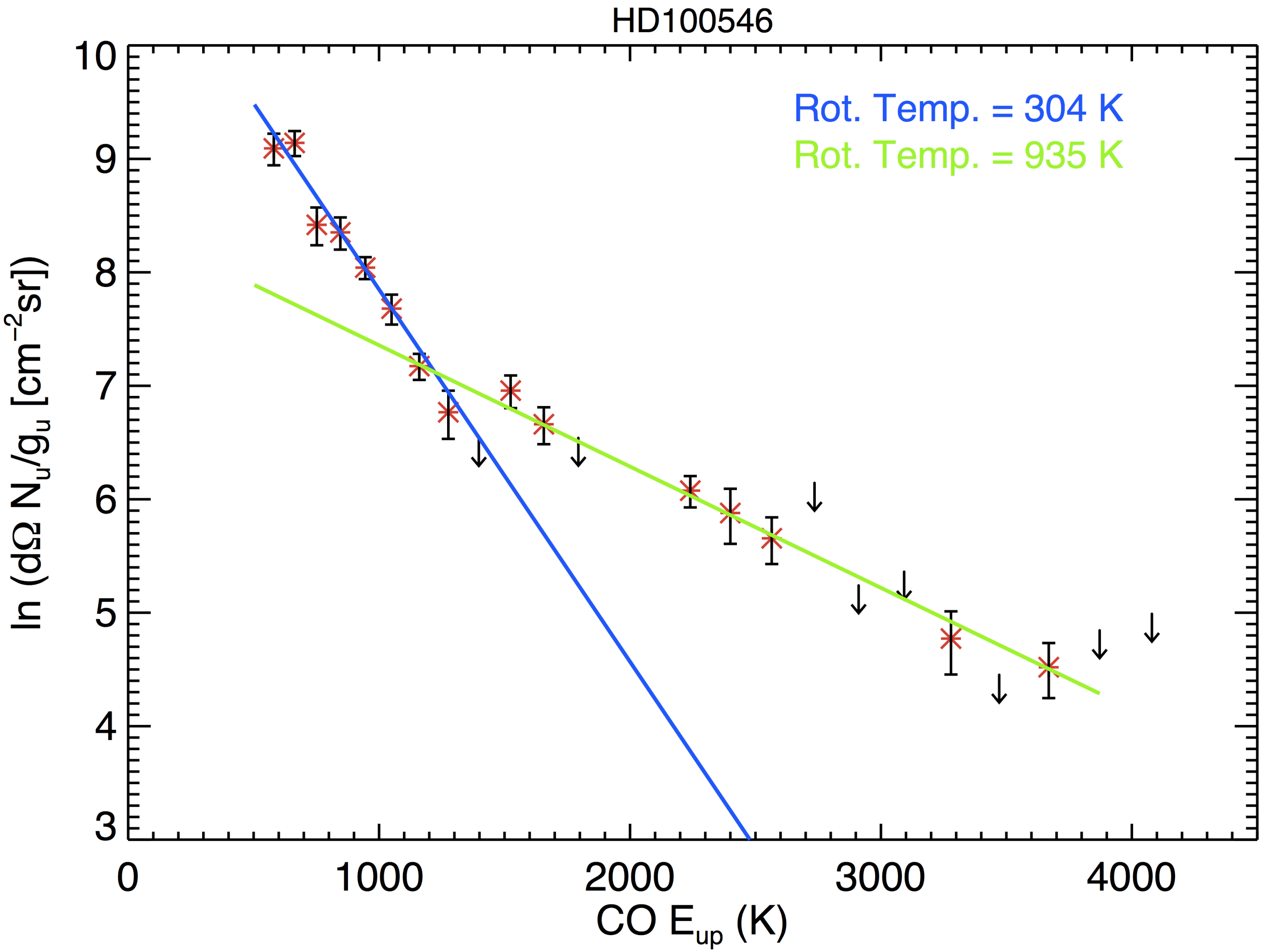

Modelling the CO ladder: PDR (*Bruderer et al. 2011*)

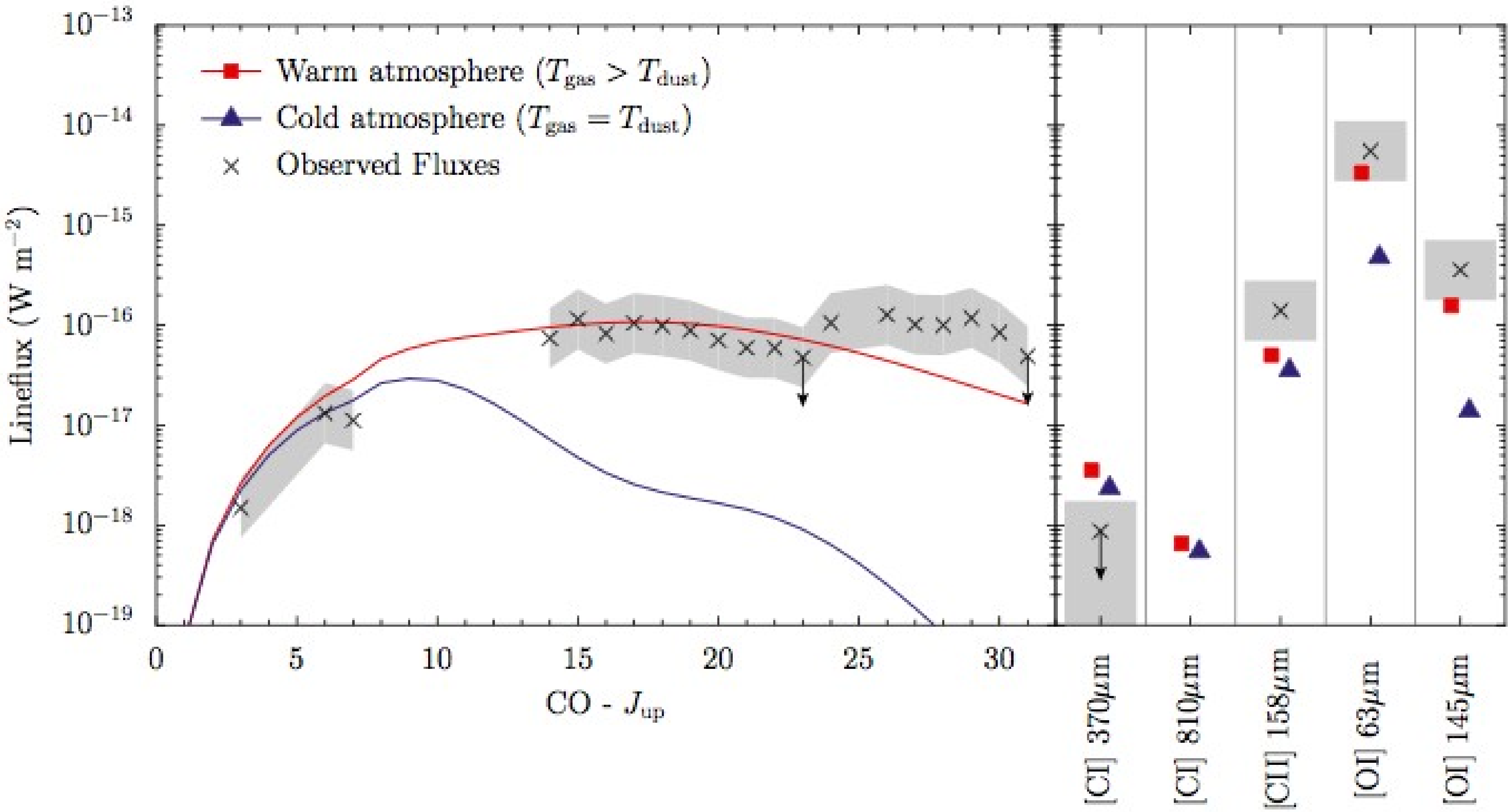

High and mid J transitions need decoupling T_{gas} & T_{dust}!

For low J transitions (region > 100 AU) not needed

Modelling the CO ladder: flaring is essential ingredient

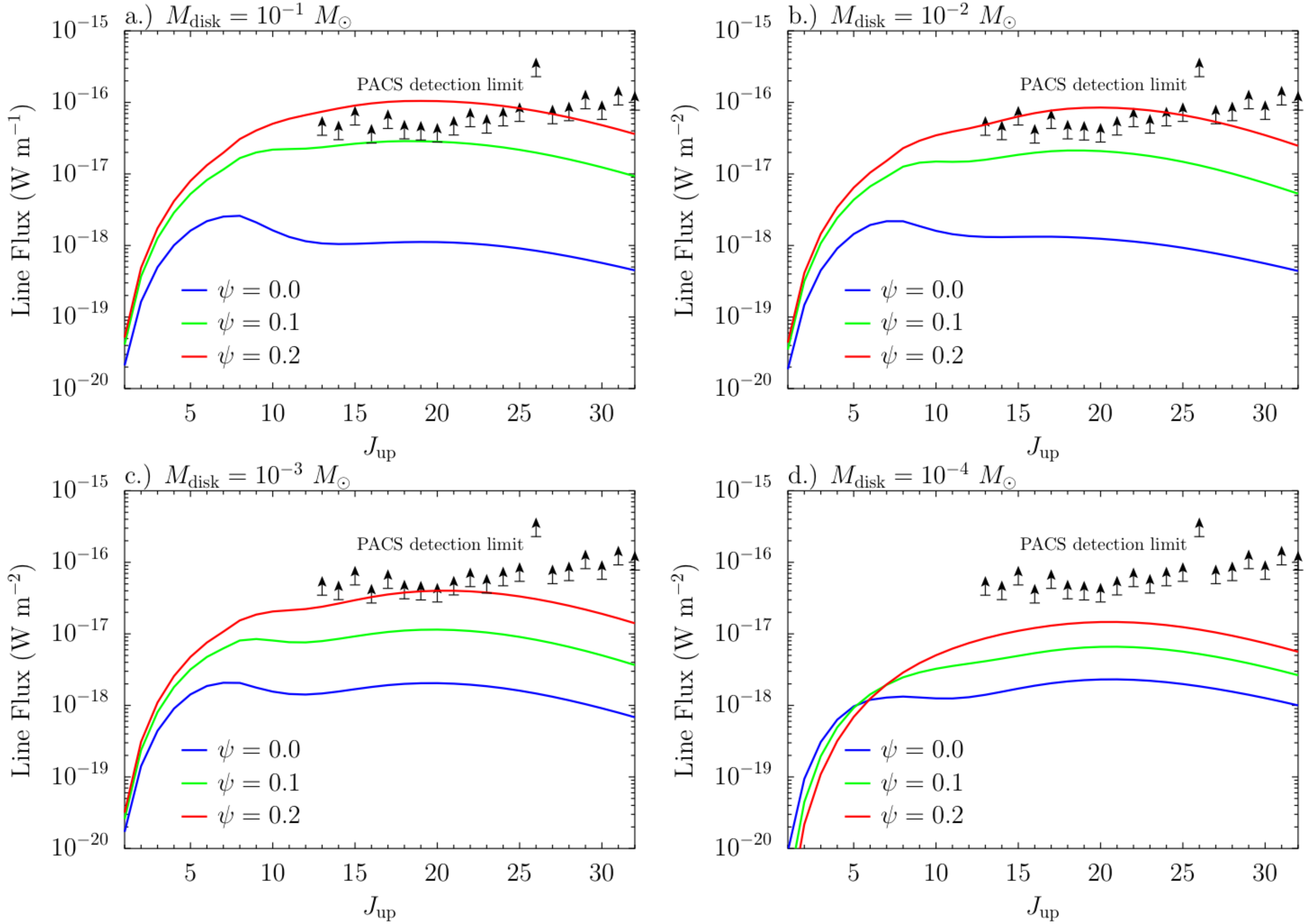

Different amount of flaring indicated by ψ. The higher the flaring, the larger the mass in warm gas. Disc mass not that critical.

Far-IR CO detections in HAEBEs: 'only' in flaring discs

SPIRE	PACS	HAEBE	Disc group	$L_{UV}/L_{\odot}$ 1150-2430 Å	L_{PAH} ($L_{\odot}$)	CO det.
→	→	*AB Aur	I	4.63	0.203	Y
		HD 35187	II	2.23	0.034	n
	→	*HD 36112	I	1.32	0.029	Y
		HD 38120	I	–	0.116	n
		HD 50138	II	–	–	n
→	→	*HD 97048	I	7.69	0.367	Y
		HD 98922	II	–	–	n
		HD 100453	I	0.29	0.038	n
→	→	*HD 100546	I	7.22	0.098	Y
		HD 104237	II	1.54	–	n
		HD 135344 B	I	> 0.11[a]	0.015	n
		HD 139614	I	0.39	0.022	n
		HD 141569 A	II/TO	6.83	0.007	n
		HD 142527	I	> 0.15[a]	0.149	n
		HD 142666	II	0.37–0.68	0.028	n
		HD 144432	II	–	0.003	n
		*HD 144668	II	1.55–2.94	–	n
	→	*IRS 48	I	4.63	0.386	Y
		HD 150193	II	8.53	–	n
→		*HD 163296	II	3.21–5.58	–	n
		*HD 169142	I	0.45	0.093	n
		HD 179218	I	–	–	n

* Inner disc clearing

* CO 18-17 detections

Transitional disc!

PACS: *Meeus et al. 2013*; SPIRE: *van der Wiel et al., submitted* (see talk Ménard)

CO in Herbig Ae/Be discs: summary

- CO mid to high J detections:
= flared discs: 5/12 sources = flat discs: 0/10 sources
Model shows that flaring is necessary to make line detectable
[a few weak detections are seen in deeper GII line spectra]

- Highest J_{up} found in HD100546, has hot inner wall

- Sources with mid-J CO detections have high UV fluxes (= sources with high T_{eff}) and strong PAH bands

- Pure rot. CO and [OI]63 line fluxes tend to be correlated

- Rotational diagram gives $<T_{rot}>$ = 271 +/- 39 K, some have (indications of) a hot component

The richest spectra: HD97048 & HD100546

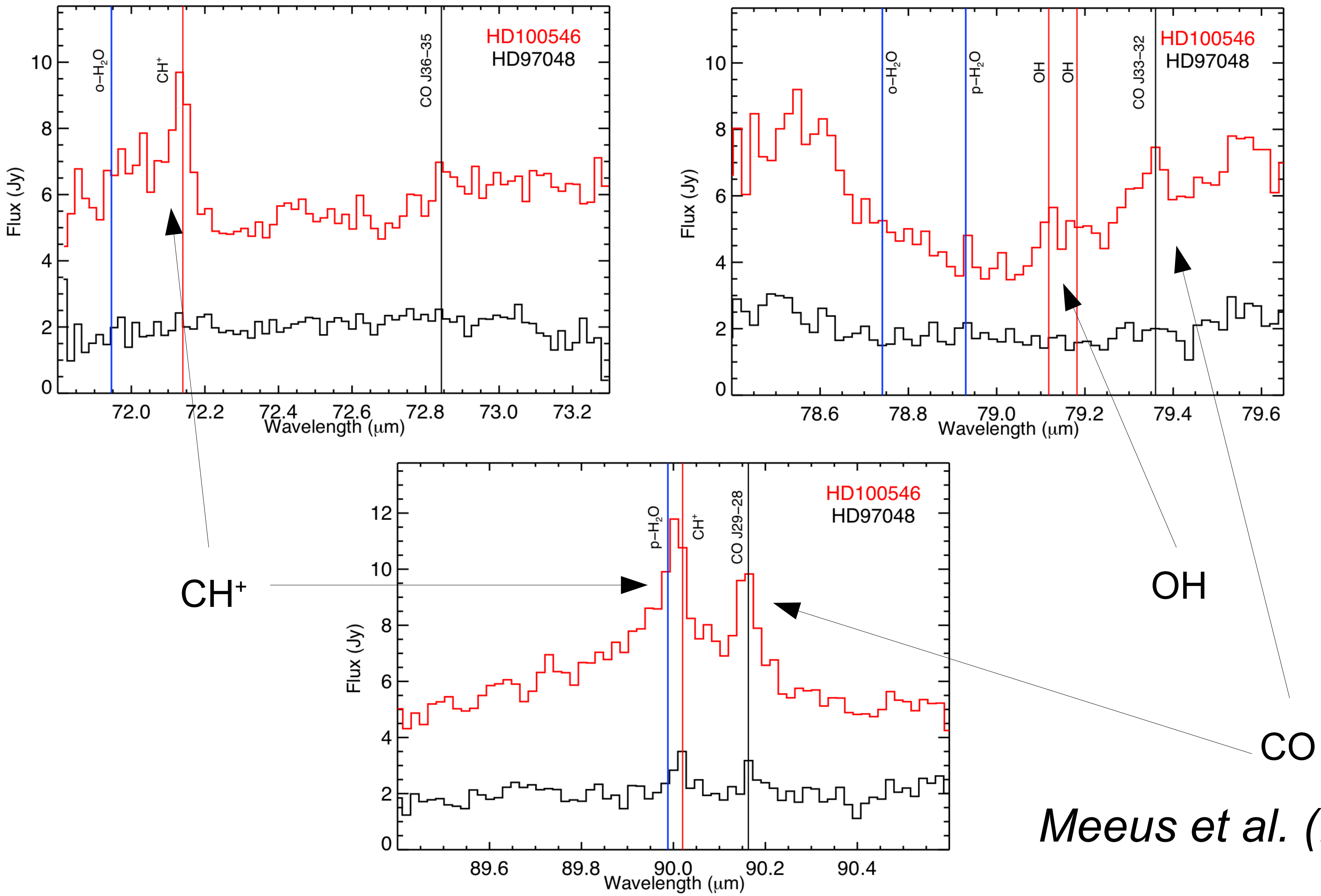

Meeus et al. (2012)

First CH^+ detection in a HAEBE

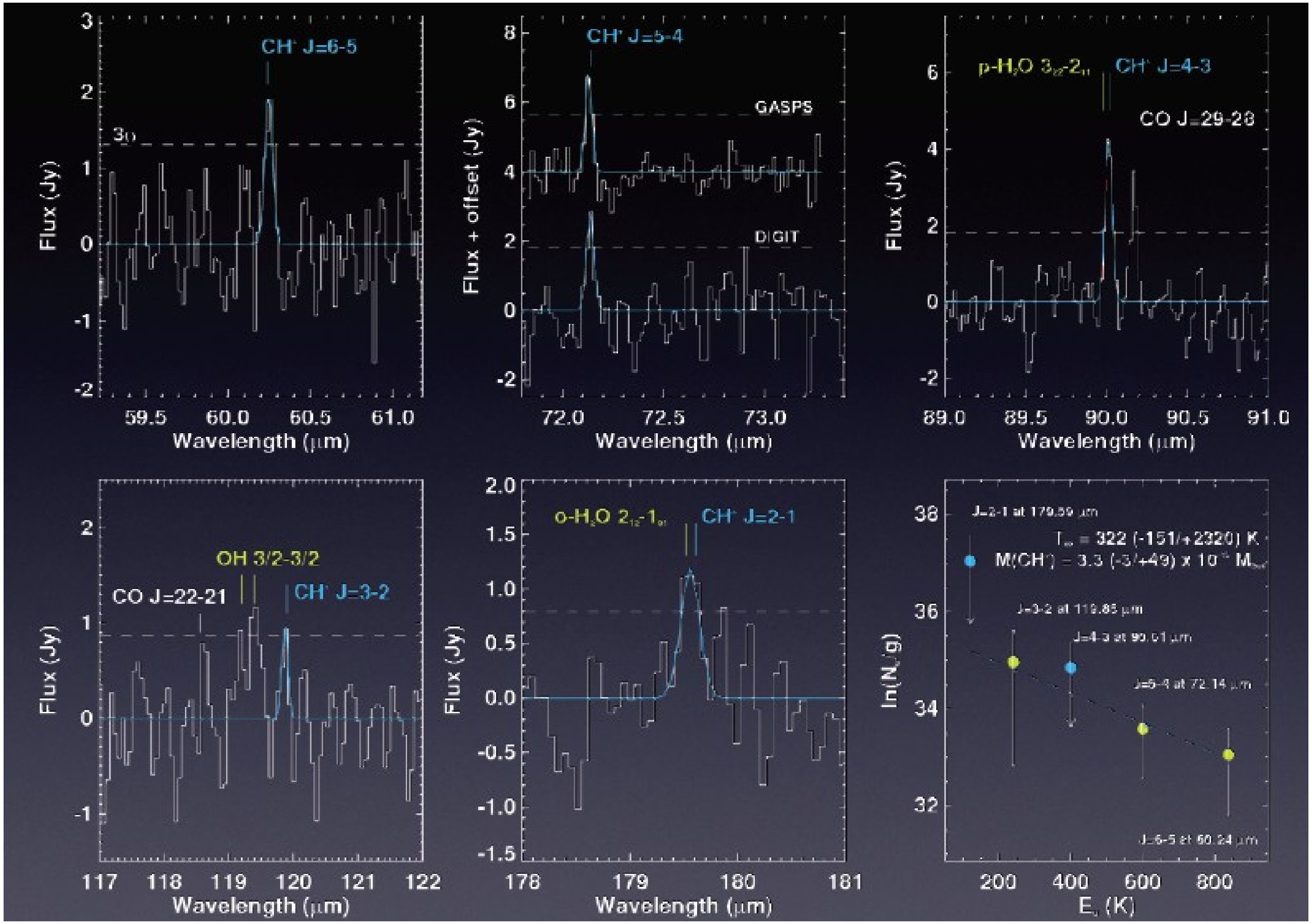

Main CH^+ formation reaction: $C^+ + H_2 \rightarrow CH^+ + H$, efficient at a few 100 K.

Thi, Ménard, Meeus et al. 2011; DIGIT data from *Sturm et al. 2010*

HD100546: modelled with ProDiMo

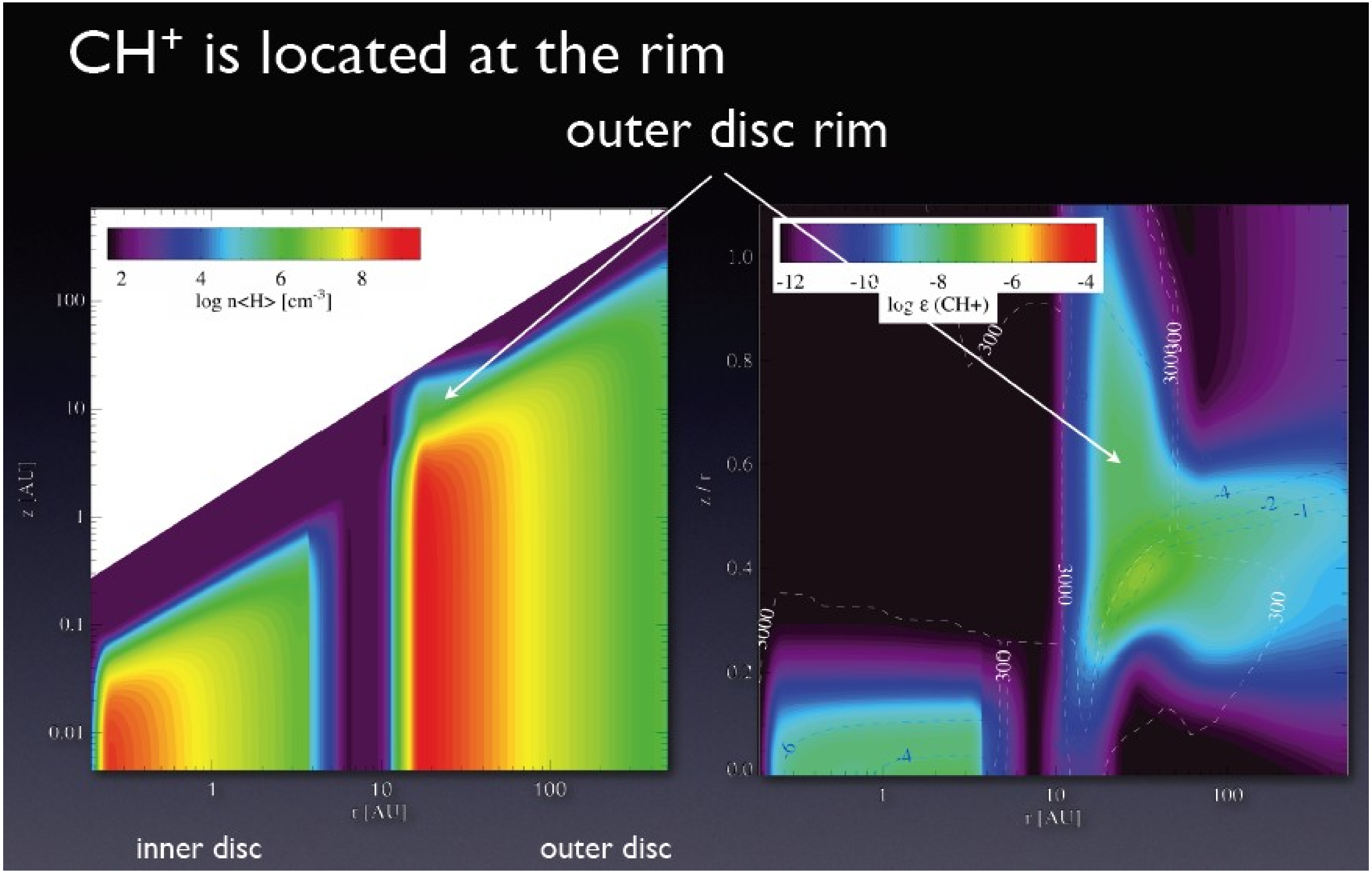

Thi, Ménard, Meeus et al. 2011

The effect of settling on the observed line flux

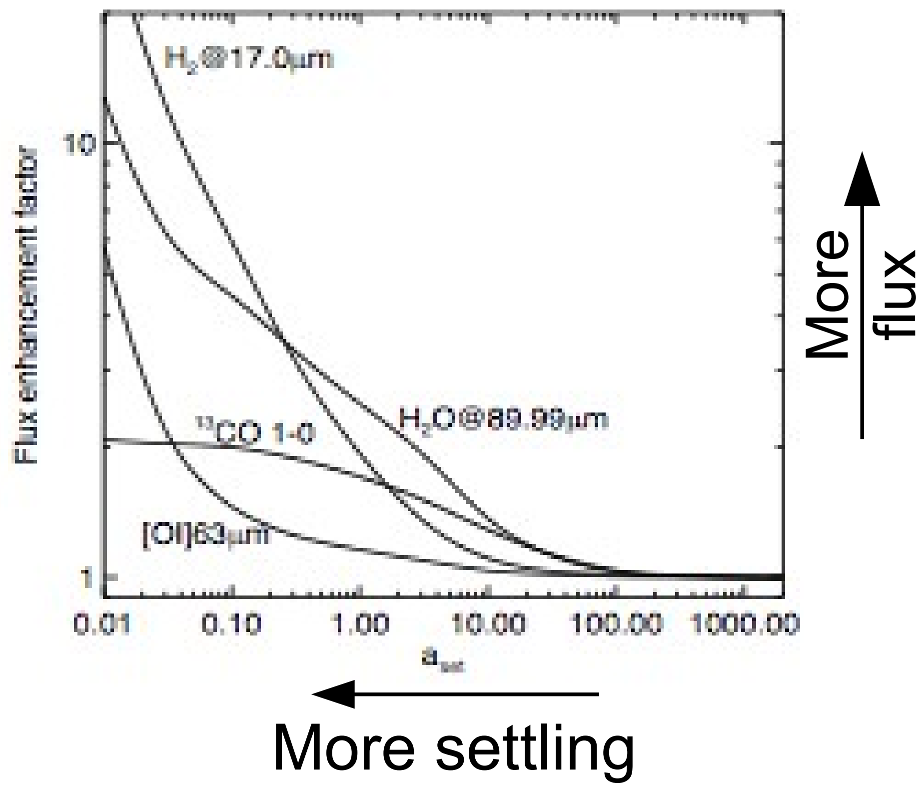

The smaller the grain size affected by settling "a_{set}" - indicating settling of grains $a \geq a_{set}$, the stronger the line flux.

When the UV photons penetrate deeper into the disc, higher densities can be reached, causing an increase in line flux.

Tilling, Woitke, Meeus et al. (2011)

HD163296: first H_2O detection in a HAEBE

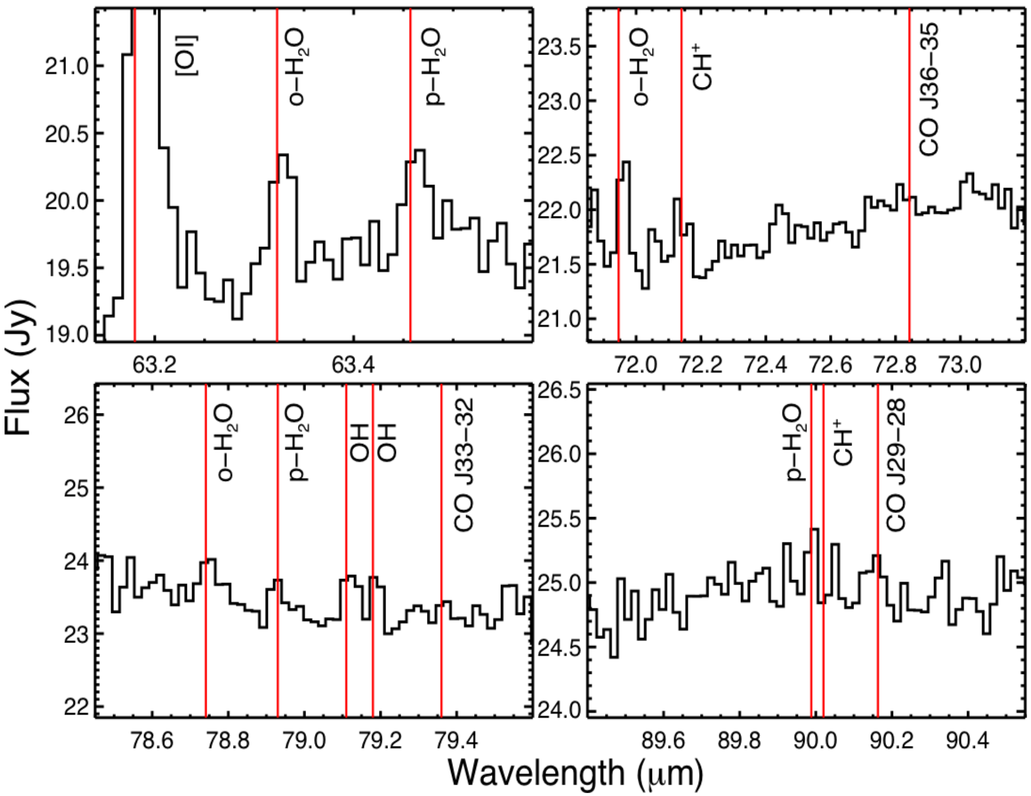

Transition	E_{up} (K)	λ_{lab} (μm)	λ_{obs} (μm)	Cont. Flux (Jy)	Line Flux (10^{-18} W/m^2)
o-H_2O $8_{18} \rightarrow 7_{07}$	1070	63.323	63.325	17.4	15.7 (3.6)
p-H_2O $8_{08} \rightarrow 7_{17}$	1070	63.457	63.465	17.4	11.1 (3.2)
o-H_2O $7_{07} \rightarrow 6_{16}$	843	71.947	71.961	18.2	13.8: (5.4)
o-H_2O $4_{23} \rightarrow 3_{12}$	432	78.742	78.751	19.6	10.7 (3.5)
p-H_2O $6_{15} \rightarrow 5_{24}$	781	78.928	78.931	19.6	<14.11
p-H_2O $3_{22} \rightarrow 2_{11}$	296	89.988	89.988	20.7	<5.0[a]
p-H_2O $4_{13} \rightarrow 3_{22}$	396	144.517	–	18.0	<12.2
p-H_2O $3_{31} \rightarrow 4_{04}$	410	158.312	–	19.1	<13.7
o-H_2O $2_{12} \rightarrow 1_{01}$	114	179.525	–	17.5	<16.7[a]
o-H_2O $2_{21} \rightarrow 2_{12}$	194	180.487	–	17.5	< 16.6
o-H_2O $7_{25} \rightarrow 6_{16}$	1100	29.85	–	17.3	43.4[b] (3.9)

Several high-excitation water lines seen.
Nothing known about low-excitation water (E_{up} < 100 K), HIFI observation too shallow.

Meeus et al., in preparation

Test models show that 1) water can form rapidly due to presence of warm gas & UV-pumped H_2, 2) only a small mass in water vapour is needed to produce observed line emission, and 3) high-excitation lines formed in inner 10 au.

H_2O detections in a HAEBEs: some thoughts

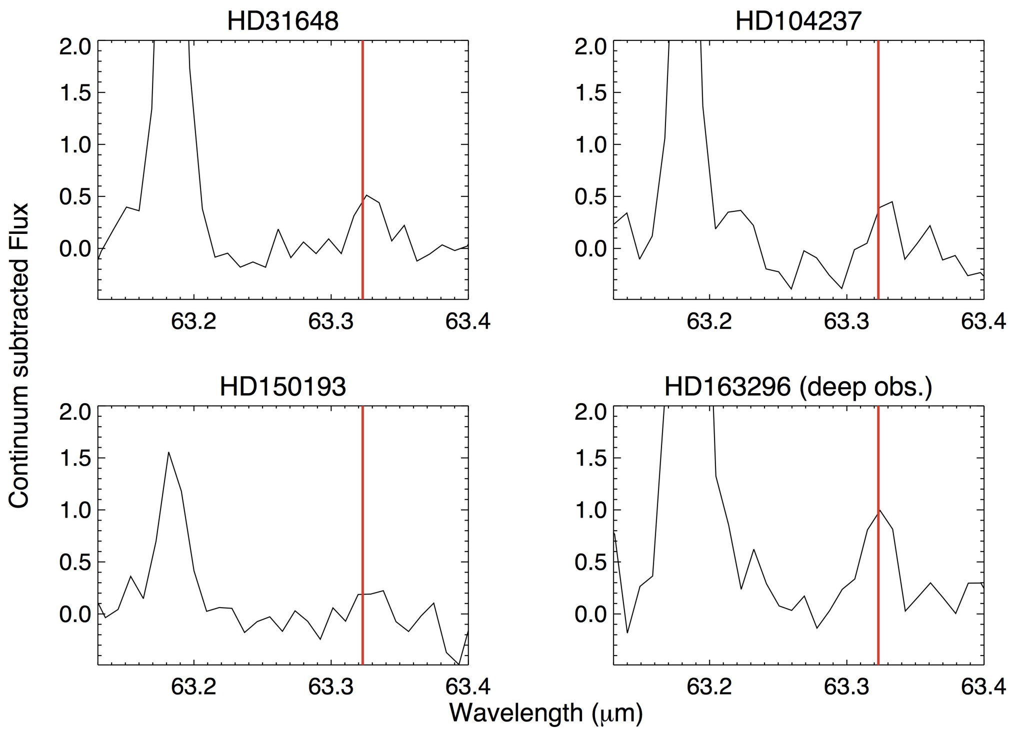

Only (tentative) detections present in flat discs.

Absence of high-excitation water lines in flared discs either due less efficient self-shielding against UV photo-dissociation or to clearing in inner disc

Lines also seen through stacking in DIGIT SED range spectra (*Fedele et al. 2012*).

! HD100546 has low-excitation water detected with HIFI, but no high-excitation lines (*Hogerheijde, private communication*).

Summary: gas in Herbig Ae discs

- [OI]63 is by far the strongest line observed, [OI]145 factor 10-20 weaker
- [OI]63 correlates with L_{UV}, amount of flaring, L_{PAH}
- CO J=18-17 only detected in 8 objects, CO ladder only in flaring discs
- OH and CH^+ detected in 2 HAEBEs
- High-excitation H_2O detected in at least 1 HAEBE, low-excitation in HD100546
- In HAEBEs, UV is important heating factor, not X-rays
- Detailed modelling of physics & chemistry crucial to understand disc but difficult to reconcile all available observations

Herbig Be discs (work in progress)

- Sample of 29 objects, most observed only in photometric mode with PACS (70, 100 & 160 μm) and SPIRE (250, 350 & 500 μm). A few in spectroscopic mode with both PACS and SPIRE (PDS 27 and R Mon)

- Auxiliary data available: SEDs and mid-IR images & spectroscopy (Verhoeff et al. 2012)

- Additional optical images (narrow & broadband) with 2.2m/CAFOS on Calar Alto

- Master thesis by MJ Jiménez Donaire (UAM)

Herbig Be discs: SEDs

PDS 27 B2?e T_{eff}=22000 K
Log L_*=3.8, M_*=9.1, d=1.25 kpc

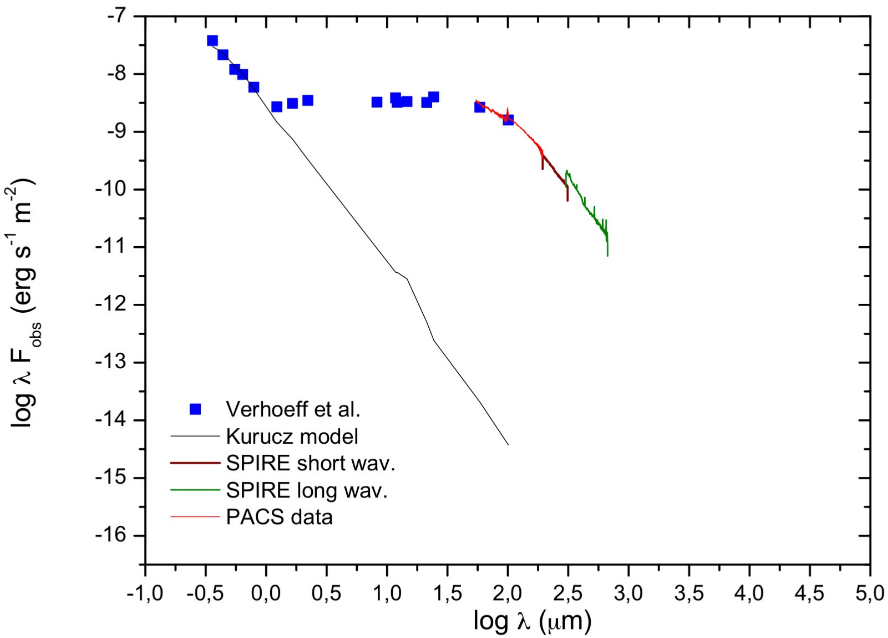

R Mon B8IIIeV T_{eff}=11500 K
Log L_*=2.1, M_*=3.4, d=0.8 kpc

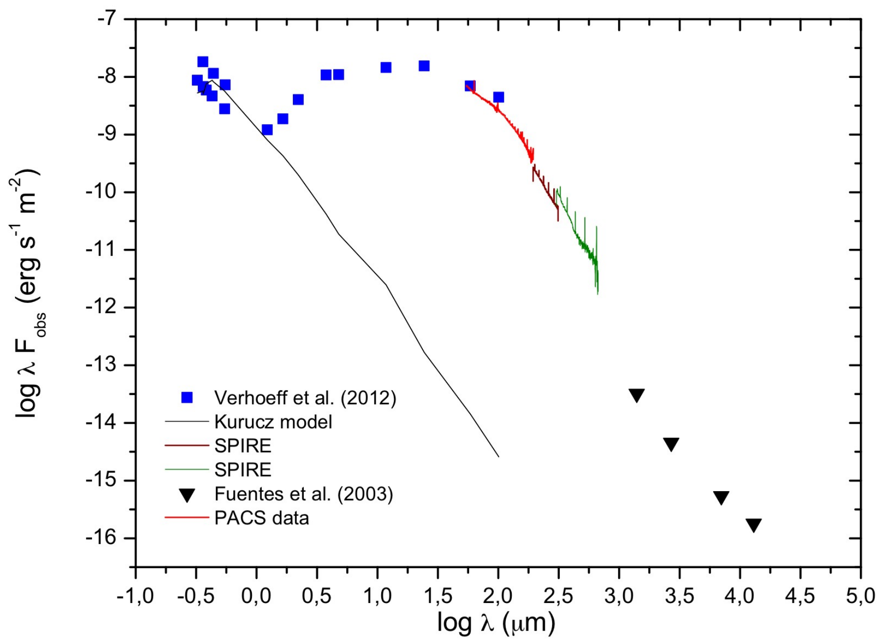

PDS 27

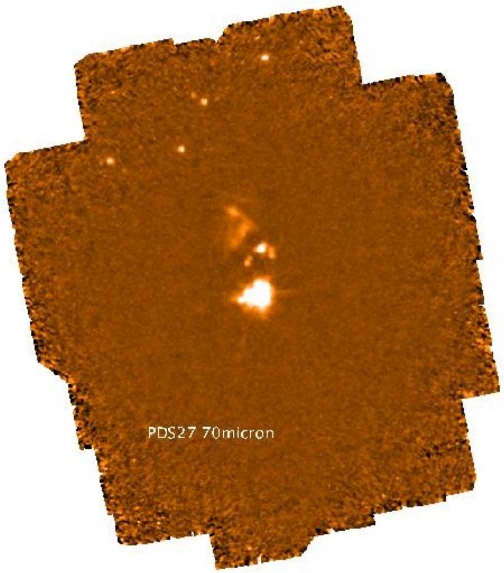

70 µm
1 pixel
= 1”

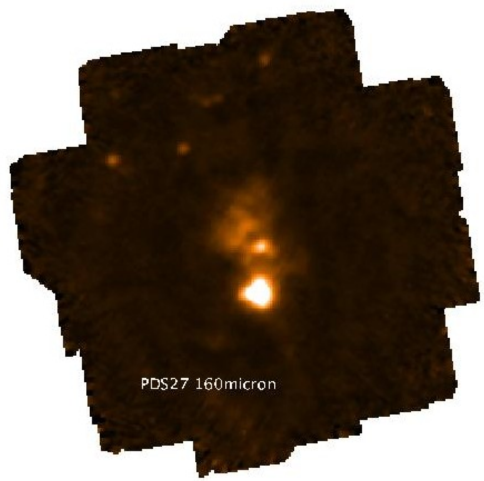

160 µm
1 pixel
= 2”

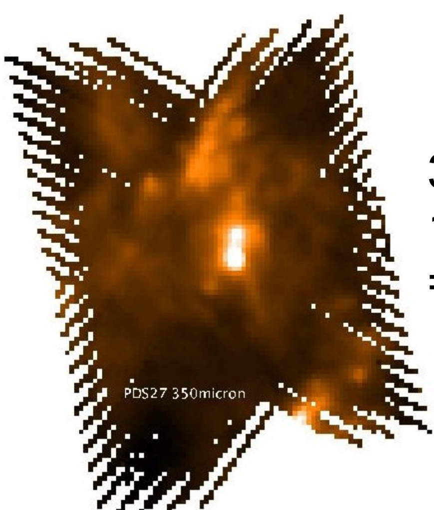

350 µm
1 pixel
= 10”

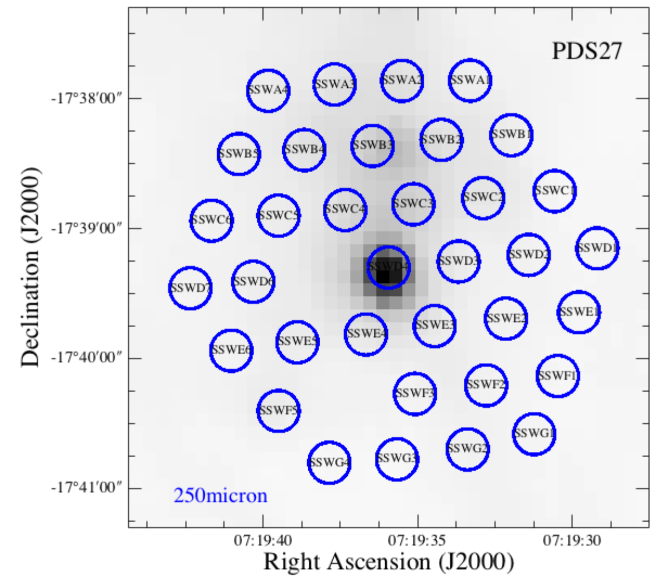

250 µm
1 pixel
= 6”

Beamsize 18”

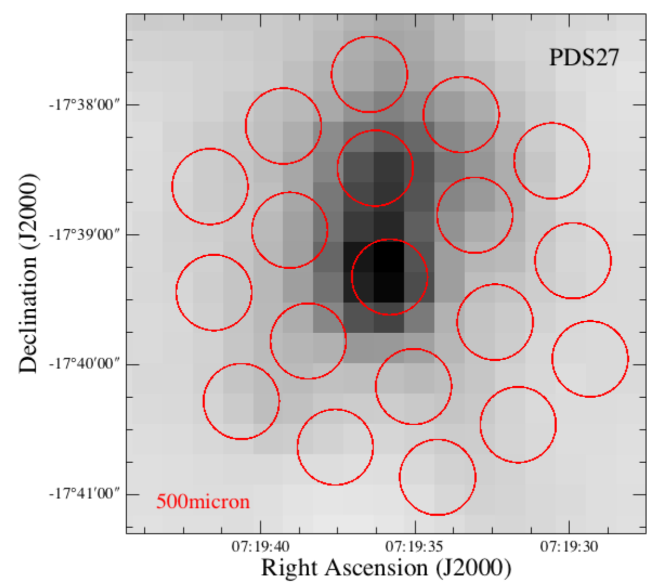

500 µm
1 pixel
= 14”

Beamsize 37”

R Mon

70 μm
1 pixel
= 1”

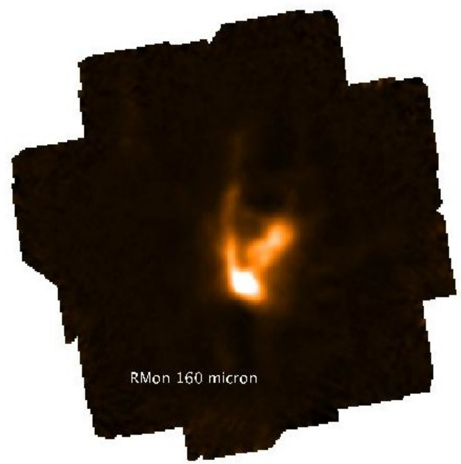

160 μm
1 pixel
= 2”

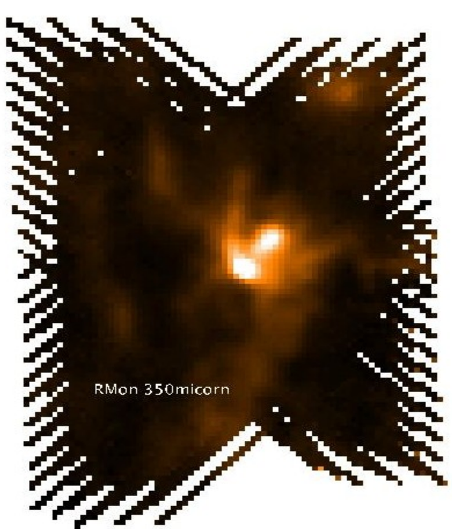

350 μm
1 pixel
= 10”

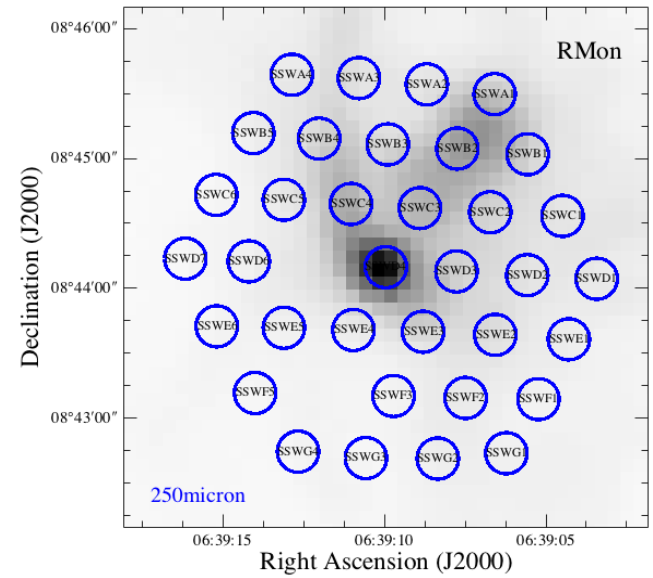

250 μm
1 pixel
= 6”

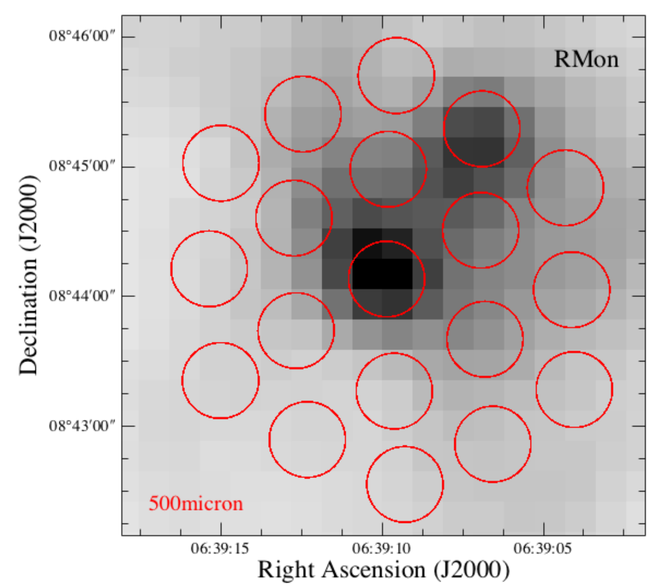

500 μm
1 pixel
= 14”

PACS and SPIRE spectra

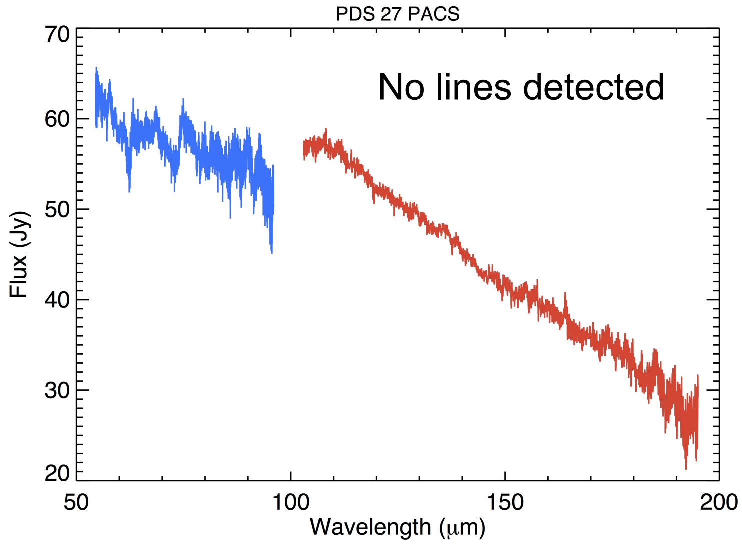

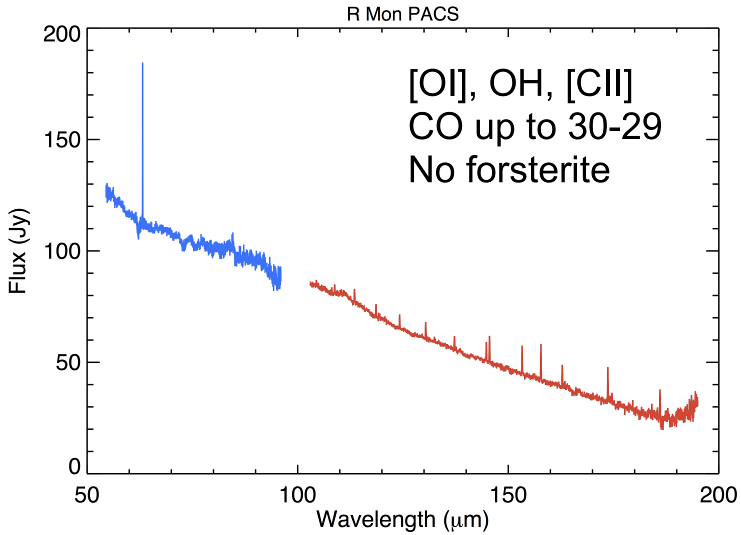

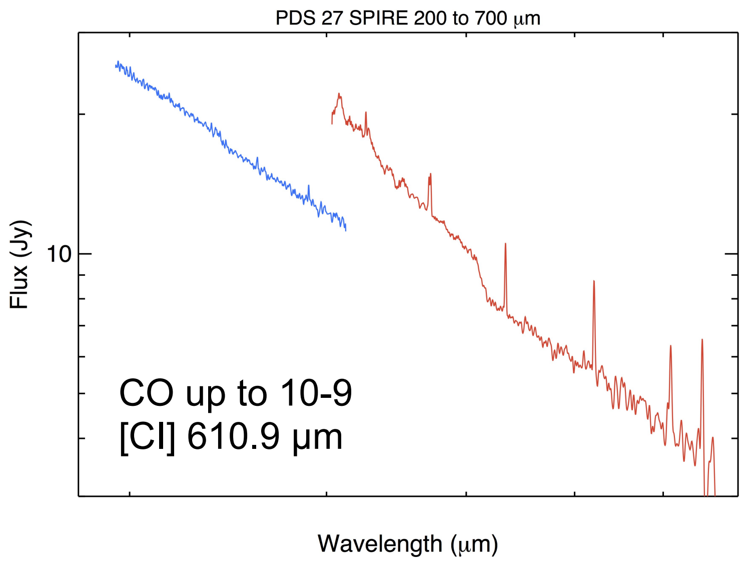

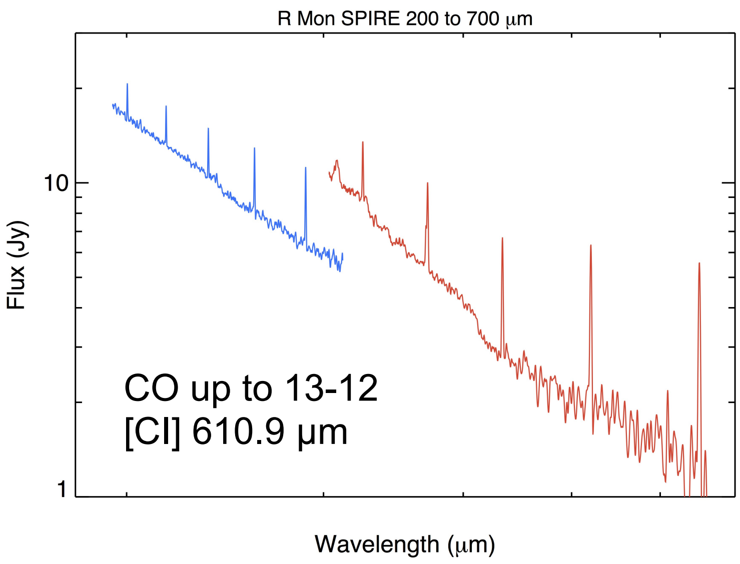

Herbig Be discs: rotational diagrams

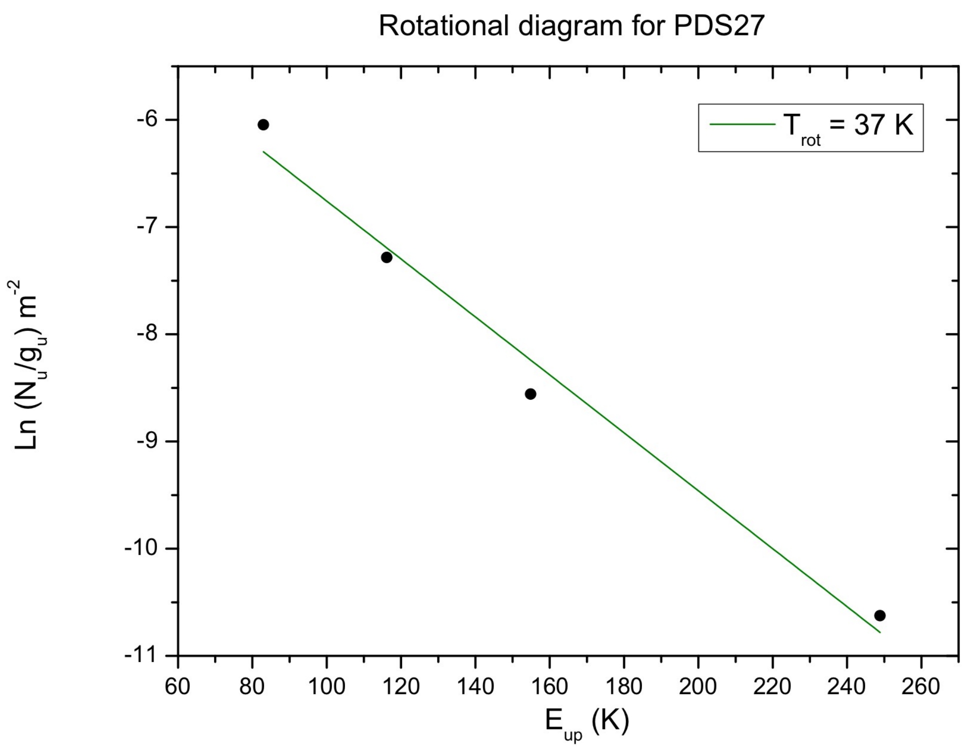

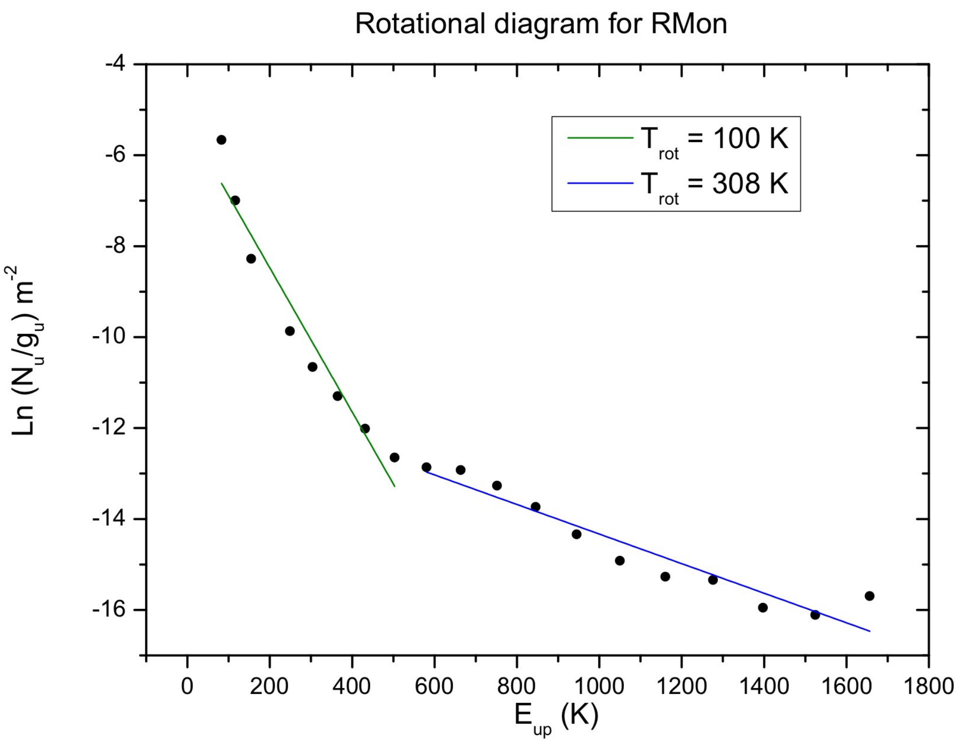

Herbig Be discs

- Detections of CO, OH, [OI], [CII], no forsterite

- Gas lines observed similarly to those found in Herbig Ae discs. The earliest spectral type has less lines

- Emission in extended regions needs to be analysed & disc parameters derived

- TBC...


The End

Ro-vibrational emission at 4.7 μm: HAEBEs

- Excitation mechanism both collisional + UV fluorescence
- Correlation found between CO line flux and PAH strength
- Self-shadowed discs: R_{in} ~ 0.5-5 AU, T_{rot} ~ 1600 - 2500 K
Dominant excitation mechanism is thermal, $T_{rot} \geq T_{vib}$
- Flared discs: R_{in} ~ 10-50 AU, T_{rot} ~ 900 - 1400 K, $T_{rot} < T_{vib}$
Dominant excitation mechanism fluorescence: L_{UV} important!

van der Plas et al. 2009 + PhD thesis, Brittain et al. 2007, 2009

Modelling the CO ladder: a small grid

Gas density

Gas Temperature

CO abundance

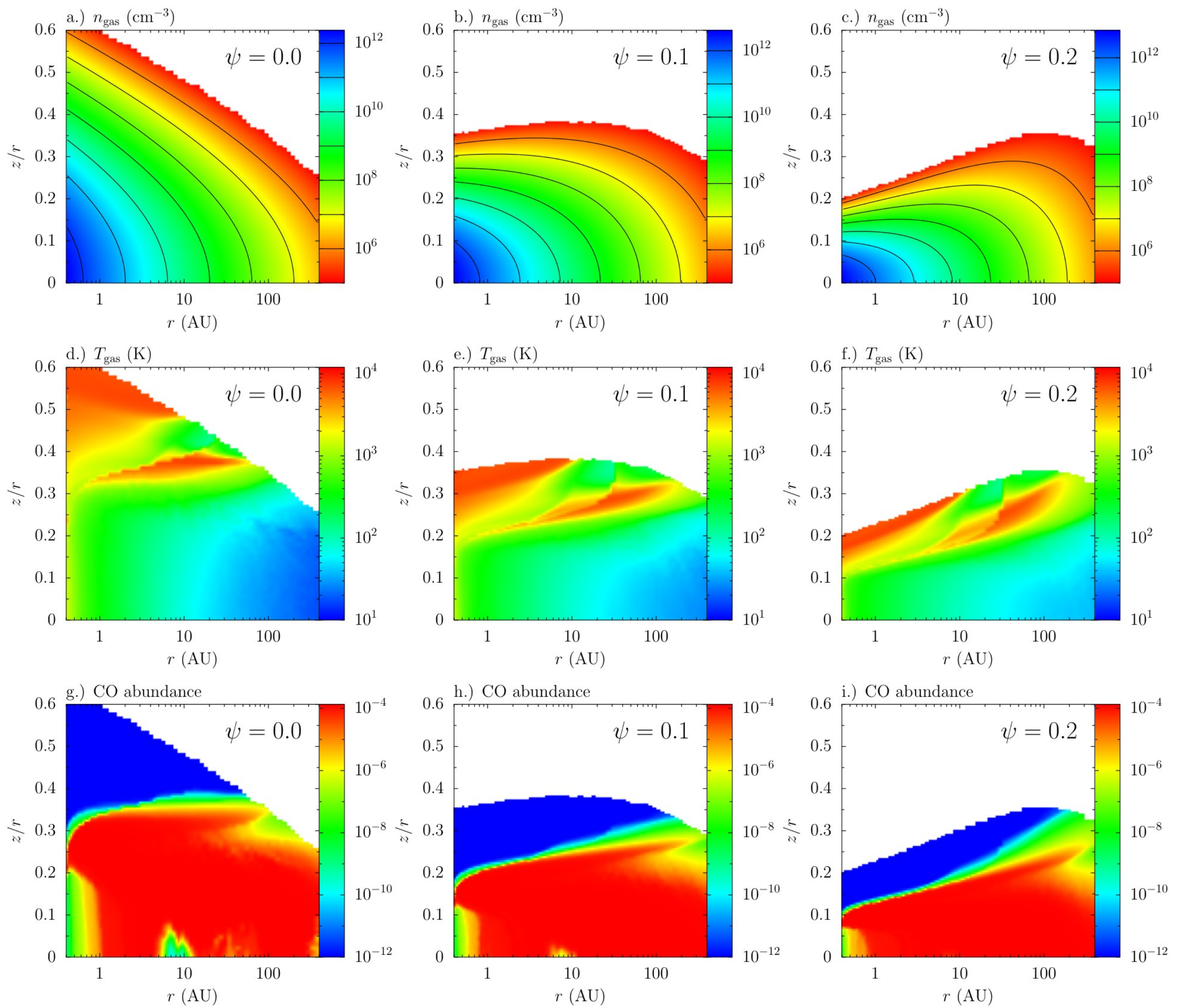

Different amount of flaring indicated by ψ

H_2 1-0 S(1) transition at 2.12 µm: only detected in HD97048 & HD100546

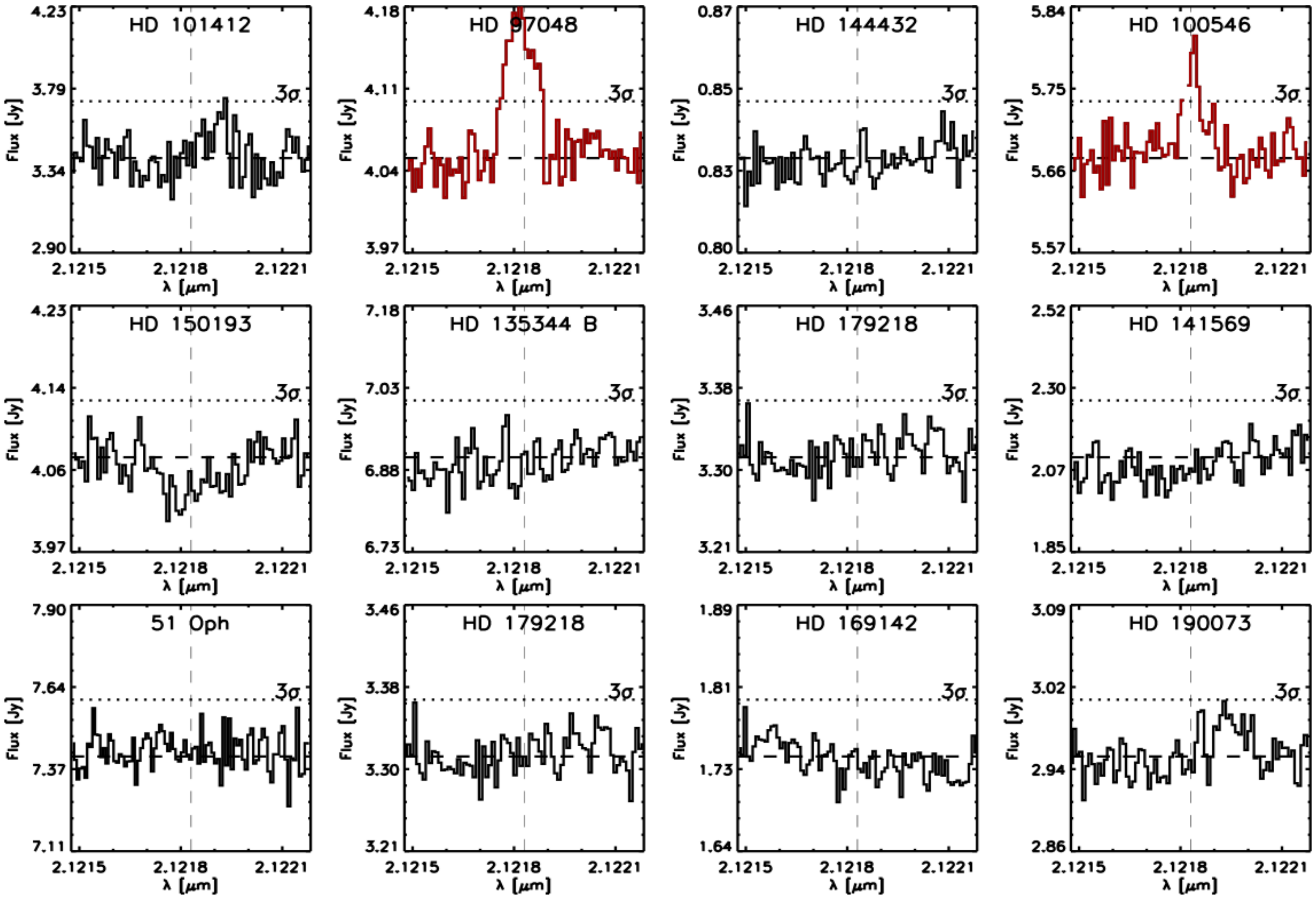

+ H_2 0-0 S(1) at 17.035 µm detected in HD97048 & AB Aur

Carmona et al. 2011, Martin-Zaïdi et al. 2007 & Bitner et al. 2007

Line (non-)detections give clues about gas in surface layers disc

When T_{gas} ~ T_{dust}, weak lines produced by thermal excitation

L_{PAH} important for thermal budget: highest AB Aur, HD97048 & HD100546

⇒ more direct heating of upper layer (more flaring)

If non-LTE, UV Fluorescence (T_{vib} > 5000 K) => T_{gas} >> T_{dust}

CO T_{vib} >> T_{rot} in flaring discs - CO T_{vib} ≃ T_{rot} in flat discs (*van der Plas*)

CO rot.-vib. at 4.7 μm:
- AB Aur, HD97048 & HD100546: **T_{Rot} ~ 1000 K**
- HD141569: **T_{Rot}~ 200 K** (kinetic T of gas) & H_2 absent

Brittain et al. 2007, van der Plas, 2009, 2012

H_2 detected only in UV-strong objects: AB Aur, HD97048 and HD100546

Location of H_2O and CO ice in HD163296's disc

The 'snowline'

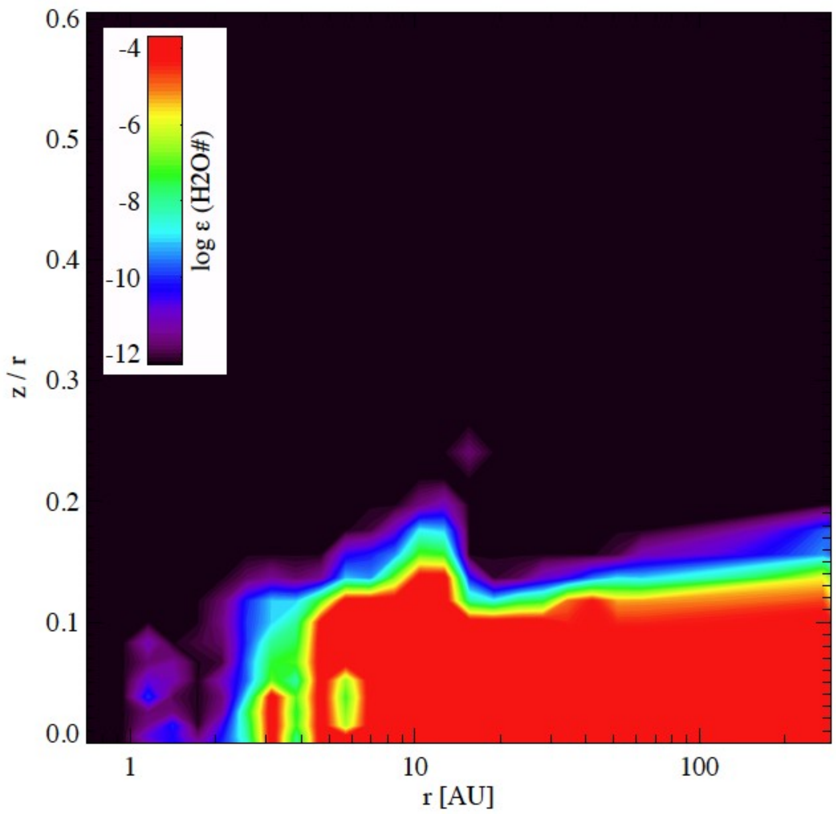

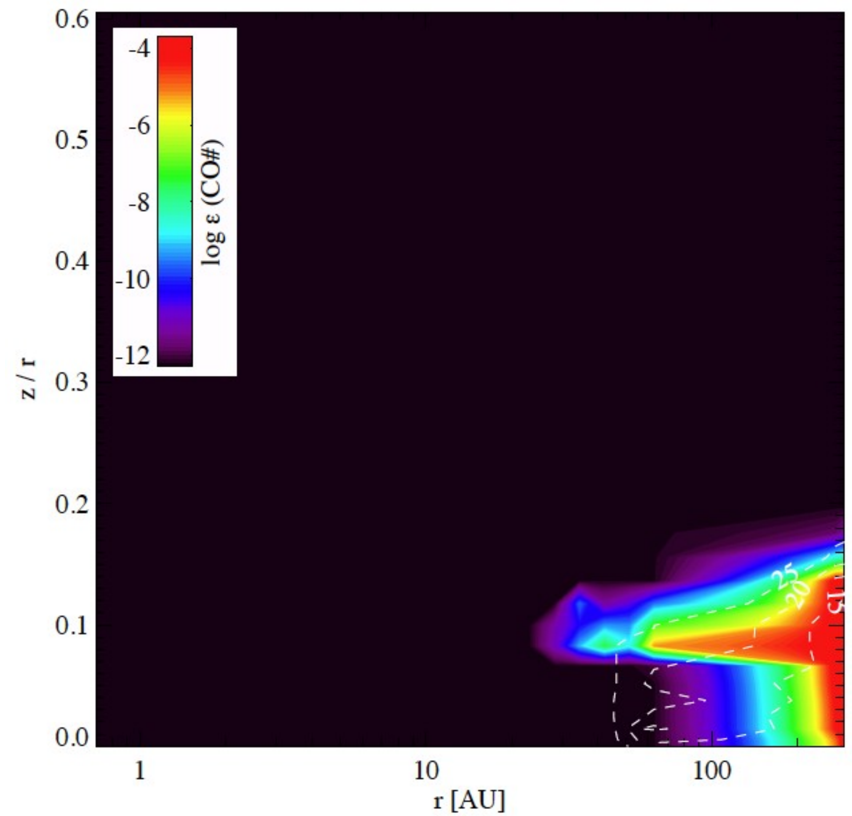

H_2O ice: from 3 AU

CO ice: from 50 AU

Origin of H_2O emission lines in HD163296

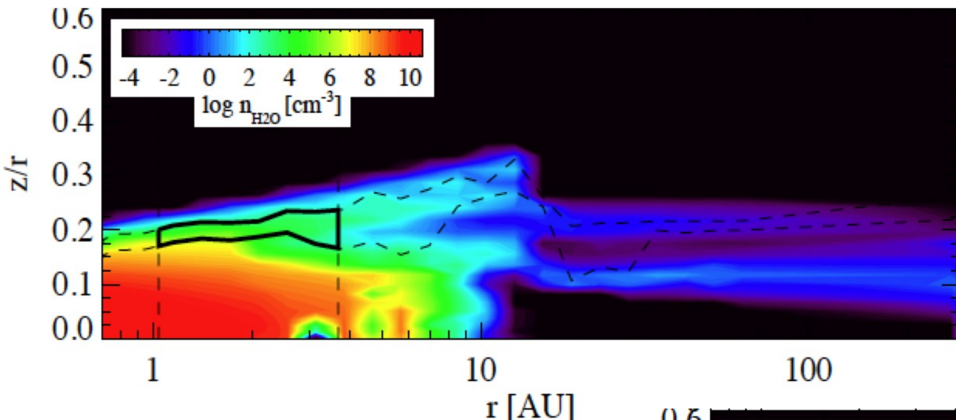

29.85 µm
E_{up} ~ 1100 K

63.323 µm
E_{up} ~ 1070 K

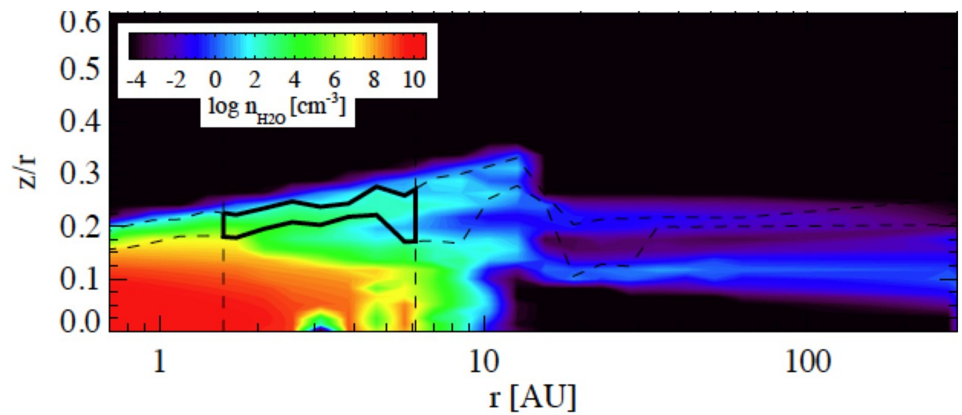

Is there cold water vapour in HAEBEs?

179.525 µm
E_{up} ~ 114 K

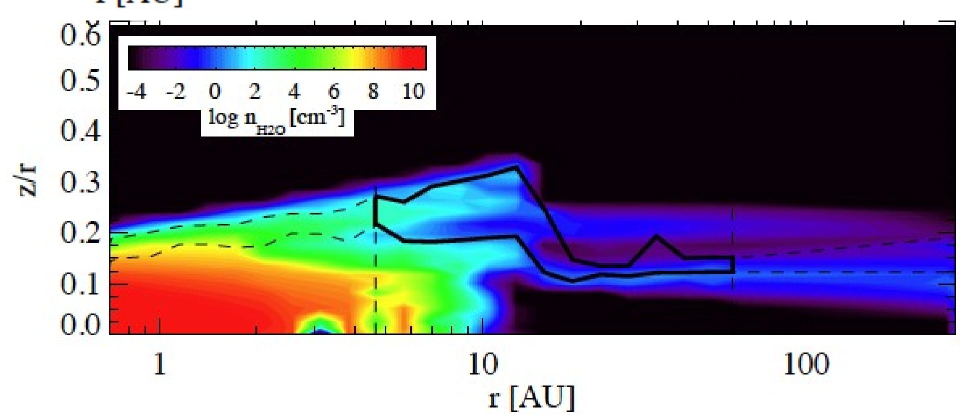

Origin of H_2O emission lines in HD163296

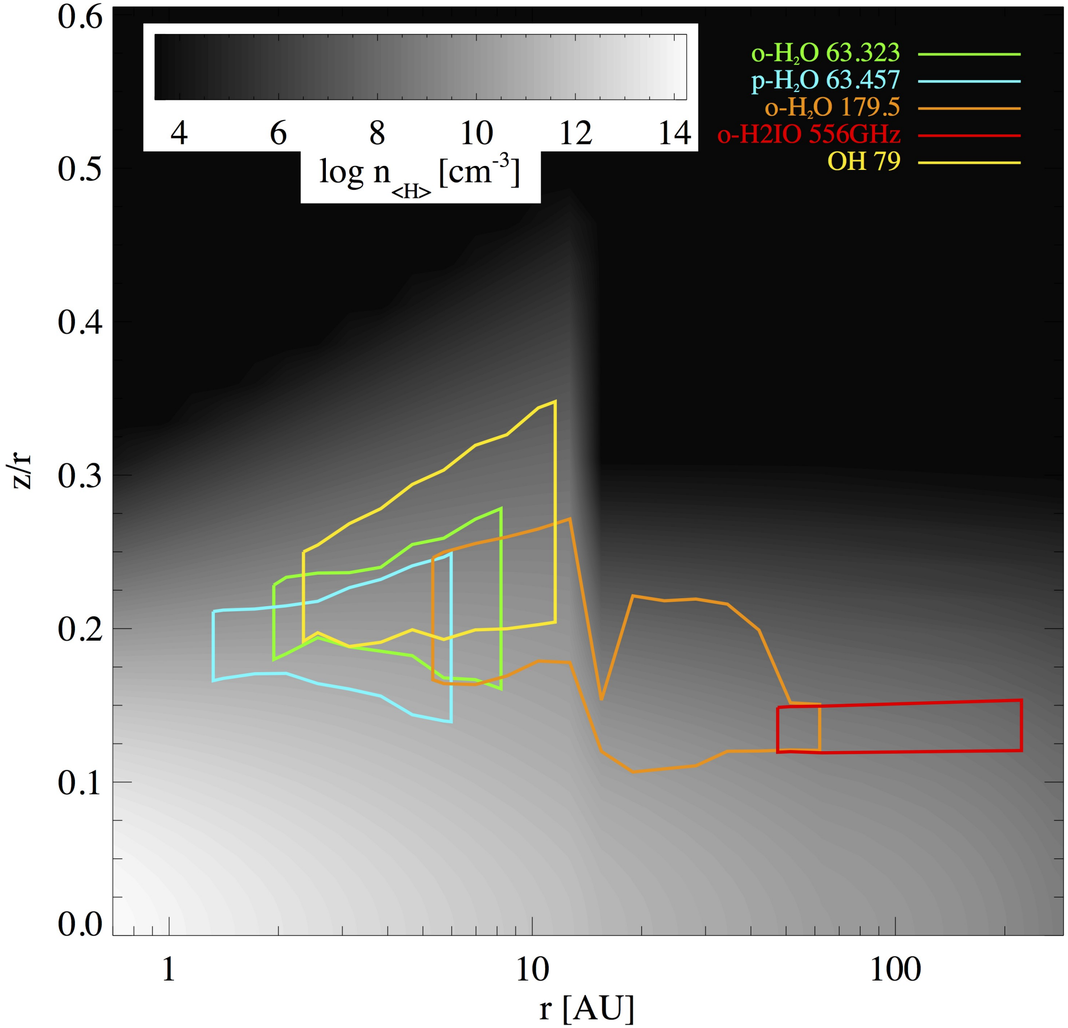

- Efficient formation of water and OH due to the presence of warm UV pumped H_2 in the disc atmosphere. OH is located higher up than water, due to the rapid photodissocation of water.
- Model only needs a small amount of mass in warm water (260 K, ~ 1 $M_{\oplus}$) to match the observed line fluxes.
- Nothing known about low excitation water (HIFI observation too shallow)
- Most of the water mass is in the form of ice (2.3 10^{-4} $M_{\odot}$), located > 3 AU.